GEOTHERMAL RESOURCE POTENTIAL FOR A PORTION OF THE SAN PEDRO RIVER VALLEY, ARIZONA

by

W. Richard Hahman, Sr.

Arizona Geological Survey
Open-File Report 81-6

April 1981

Arizona Geological Survey
416 W. Congress, Suite #100, Tucson, Arizona 85701

Funded by the U.S. Department of Energy
Contract Number DE-FC07-79ID12009

This report is preliminary and has not been edited or reviewed for conformity with Arizona Geological Survey standards

RECONNAISSANCE STUDY

GEOTHERMAL RESOURCE POTENTIAL OF A PORTION OF THE SAN PEDRO RIVER VALLEY

INTRODUCTION

A preliminary investigation of the geothermal resource potential of the San Pedro River valley was undertaken the latter part of 1980. The area of investigation is situated in Pinal, Pima and Cochise counties, Arizona. It extends from the town of Mammoth, Pinal County, south-southeast along the river valley to just north of the Johnny Lyon Hills, an area comprising 2331 km^2 (900 mi^2).

With the exception of mining and smelting activities in the Mammoth-San Manuel area, the primary business in the valley is agriculture, cattle ranching and forage crops. The majority of the irrigation, livestock, and domestic wells are along the bed of the San Pedro River, an ephemeral stream that flows northward from its headwaters in Mexico. The wells generally vary in depth from 24 m (80 ft) to 36 m (120 ft) and essentially produce from the subsurface river flow.

In the Mammoth-San Manuel area there are some warm artesian wells that vary in depth from approximately 244 m (800 ft) to 457 m (1500 ft). The warmest temperature measured in these wells was 40°C (104°F).

GENERAL GEOLOGY

The San Pedro River valley lies along the western edge of the Mexican Highland section of the Basin and Range province (Fenneman, 1931). Fenneman (1931) describes this section of the Basin and Range province as "approximately half mountain and half plain" with a northwestward trend. In this report the studied portion of the San Pedro River valley is bounded on the west by the Santa Catalina and Rincon mountains and on the east by the Galiuro and Winchester mountains. Figure 1 is the regional geology of the study area compiled from the Geologic Map of Arizona (1969) by Wilson, Moore and Cooper.

Both Heindl (1963) in the Mammoth-San Manuel area and Montgomery (1963) in the Tres Alamos wash (just south of the Johnny Lyon Hills) area show the San Pedro River valley to be a complex graben structure trending approximately N. 30° W. This graben structure is step-faulted downward toward the center of the basin from the eastern and western bounding mountain ranges.

The high angle normal faulting commenced approximately 15 m.y. ago at the advent of the Basin and Range disturbance (Shafiqullah and others, 1980) during middle to late Miocene. The major faulting that formed the graben in the San Pedro River valley had probably concluded by middle to late Pliocene with only minor structural adjustments since that time.

Scarborough (1975) postulated a doming of the San Pedro basin in late Pliocene time that, coupled with the steady downcutting of the San Pedro River, has left the Pliocene and Pleistocene sedimentary deposits at elevations higher than would normally be expected. The apparent absence of post-Pliocene faulting (Menges, 1981) tends to give credence to the doming hypothesis.

Figure 3 is a simplified stratigraphic column of the Cenozoic lithologies present in the area of investigation (Menges, pers. commun., 1981). The thicknesses of these units vary throughout the San Pedro valley. The brief descriptions of the lithologic units were synthesized from Heindl (1963); Montgomery (1963); Krieger (1974); Krieger et al., (1974); and Scarborough and Wilt (1979). The reader is referred to these writers for more detailed descriptions and for an understanding of the magnitude of the correlation problem.

The pre-Cenozoic stratigraphy (Fig. 4) crops out on the west side of the valley and along the east flanks of the Santa Catalina Mountains. The majority of the study area was mapped by Cunningham and Hahman in 1963.

The west-northwest-trending Mogul fault plays a key role in the geology of the San Pedro River valley in the area of investigation. The Mogul fault appears to be part of the Texas zone (Rehrig and Heidrick, 1976). For a dis-

CENOZOIC

STRATIGRAPHIC COLUMN
SAN PEDRO RIVER VALLEY
STUDY AREA

Formation Name	Yrs x 10^6	Description
Unnamed gravels	$\leq$ 2	Pleistocene and Recent: river gravels and alluvial fan deposits (possibly the informal Tres Alamos Fm of Montgomery, 1963).
Quiburus Fm	4-7	Pliocene: fine-grained lacustrine deposits with some fluvial deposits in places overlain by unnamed Pleistocene gravels and alluvial fans. The main sedimentary unit exposed in the river valley in the area of study.
Galiuro volcanic	22-29	Oligocene and Miocene: rhyolite to andesite lava flows and ash flow tuffs.
"Teran" beds	$\geq$ 27	Oligocene: fanglomerates, sandstone, shale and mudstone with a centrally situated andesite

Figure 3

PRE-CENOZOIC

STRATIGRAPHIC COLUMN

SAN PEDRO RIVER VALLEY

STUDY AREA

ERA	PERIOD & FORMATION		YRS x 10^6
Cenozoic	See Figure 2	unconformity	
Mesozoic	undifferentiated volcanic rocks arkoses red beds	unconformity	65
Paleozoic	Pennsylvanian Horquilla Ls	unconformity	247 341
	Mississippian Escabrosa Ls	unconformity	367
	Devonian Martin Fm	unconformity	416
	Silurian Ordovician missing	unconformity	510
	Cambrian Abrigo Fm Bolsa Quartzite	unconformity	570
Precambrian younger	Troy Quartzite Mescal Limestone Dripping Springs Qtzite	unconformity	1420
older	Oracle granite		

Figure 4

cussion of the Texas zone or lineament the reader is referred to Schmitt (1966); Swan (1976); and Titley (1976). For a discussion of the Mogul fault and the regional geology affecting the San Pedro River valley the reader is referred to Durning and Davis (1978); Silver (1978); and Drewes and Thorman (1978).

The Mogul fault, a left-lateral, normal fault, is situated at the northern end of the Catalina Mountains and south of Oracle. It strikes approximately N. 70° W. and dips steeply to the southwest. Durning and Davis (1976) indicated a dip of 55° SW, a heave or horizontal displacement component of 1500 ft, and a minimum throw or vertical displacement component of 4500 ft.

Drewes and Thorman (1978, Fig. 1) appeared to correlate the Mogul fault in the northern end of the study area with Cooper's (1958) Antelope Tank fault, which passes north of the Johnny Lyon Hills and south of the Teran basin in the southern end of the study area. This apparent correlation seems tenuous. Drewes and Thorman (1978) indicated that both faults have the same relative movements. However, Cooper (1958) and Durning and Davis (1978) indicated the relative movements on the two faults are opposite to each other. Projections of their strikes on the USGS 2° Tucson map indicate that the faults are probably parallel to each other. Examination of the current magnetic (Sauck and Sum-

ner, 1971) and gravity (Lysonski, Aiken and Sumner, 1981) (Fig. 5) data do not indicate any physical connection of the two faults under the valley fill. The gravity and magnetic data indicate the projected traces of the two faults are obscured by the east and west basin bounding faults and the Morenci lineament, as well as by the Galiuro volcanic rocks in the basin. The Antelope Tank fault is projected northwestward into the vicinity of Hookers Hot Springs where it is apparently obscured by the Oligocene-Miocene Galiuro volcanic rocks and the Morenci lineament.

The vertical movement on the Mogul fault has apparently controlled preservation of the Paleozoic lithologies in the San Pedro River valley (Titley, 1976). On the north-northeast (upthrown) block the Paleozoic section is not preserved. Where the Precambrian rocks are exposed, they are in contact with and overlain by Mesozoic and Cenozoic (?) rocks. On the downthrown block the Paleozoic section is preserved on the east side of the Catalina Mountains. East of the study area in the Winchester Mountains, on the north side of the downthrown Antelope Tank fault, Paleozoic sediments are observed deposited on Precambrian basement rocks. Therefore, the Mogul and Antelope Tank faults do not appear to be the same fault.

The gravity and magnetic data indicate the Black Hills, a Paleozoic outcrop south of San Manuel and north of the projected southeast extension of the Mogul fault, to be root-

less. Therefore, the Black Hills are inferred to be a slide block from the Catalina Mountains rather than a small horst in a complex graben.

To further complicate the geological picture, the Morenci lineament (Fig. 5) passes through the San Pedro valley in a northeast-southwest direction (Chapin et al., 1978; and Witcher, pers. commun., 1981). The lineament, approximately 8 to 12 km (5 to 8 mi) wide in the study area, passes through the Galiuro Mountains just to the north of Hookers Hot Springs, the southern edge being reflected in the "dog leg" to the southwest along Pine Ridge and Rockhouse Canyon, T. 12 S., R. 21 E. In the Galiuro Mountains the Morenci lineament passes south of Bassett Peak, the northern boundary being in the vicinity of the west-trending portion of Redfield Canyon. In the basin, the lineament passes south of Redington and north of Cascabel exiting the valley in the vicinity of Piety Hill and Mineta Ridge. The lineament zone passes through Redington Pass, which divides the northern Santa Catalina Mountains from the southern Rincon Mountains, and could well account for the southwestward extension of the northern Rincon Mountains.

Witcher (1981) describes the Morenci lineament in Arizona as follows:

"(1) The San Francisco River changes direction near

Glenwood and follows the lineament.

"(2) The Gila River changes course south of Clifton and follows the lineament through the Peloncillo Mountains.

"(3) Nearly every mountain range and basin show a "dog leg" at the lineament intersections in southeastern Arizona.

"(4) Every other mountain block is structurally high--three of four of these blocks are metamorphic core complexes (Davis and Coney, 1979), with the easternmost in Arizona.

"(5) Sediment-filled basins traversed by the Morenci lineament have the lowest and most intense residual Bouguer gravity anomalies in southeastern Arizona (Lysonski and others, 1980). These anomalies are on or immediately adjacent to the lineament. The anomalies are interpreted to indicate that these basins have the greatest thicknesses of basin-filling sediments, which may signify the greatest structural displacements.

"(6) <u>Every</u> hot spring with a temperature <u>greater than 40°C</u> in southeastern Arizona occurs within 19 lateral kilometers of this lineament. Sixty percent of all reported warm and hot springs (>30°C) in Arizona occur within 48 kilometers

of this lineament (see Fig. 3 of Witcher).

"(7) An inferred, northeast-striking structural zone crosses the Tucson area on trace of the Morenci lineament. Gravity and resistivity data suggest a fault on the north side of the Sierrita Mountains (Vroman, 1976; Davis, 1971). En echelon faults are observed along the northeast-trending Black Mountain (Percious, 1968). An aeromagnetic anomaly follows the same trend across the Tucson basin (Sauck and others, 1971). A groundwater "fall" also occurs along this trend in the Tucson basin and suggests an impermeable fault boundary (Davidson, 1973). All of these features are on strike with one another.

"(8) Three different clusters of major Laramide copper deposits occur within 24 kilometers of the Morenci trend where it transects linear discontinuities of the Texas Zone; they are the Pima Mining District, Safford Mining District, and the Morenci Mining District."

The intersection of the Morenci lineament with the Antelope Tank fault zone and/or the basin graben faults are postulated to provide the structural origin of Hookers Hot Springs.

In the San Pedro Valley the gravity data indicate that the basin has been filled with Oligocene-Miocene Galiuro volcanic rocks. This thick sequence of volcanic rocks was downfaulted and probably simultaneously filled the basin graben structure during its formation.

A minimum depth to the Precambrian basement, north of the projected trace of the Mogul fault, may be estimated by calculating the combined thicknesses of the Quiburus Formation and the Galiuro volcanic pile assuming there are no older Cenozoic formations under the Galiuro volcanic rocks and that the Paleozoic section is no longer preserved on the northern side of the Mogul fault. Heindl (1963) postulated a thickness 518 m (1700 ft) of Quiburus Formation in the Mammoth-San Manuel area. Hahman, this report, estimated a minimum thickness of 1070 m (3500 ft) of exposed Galiuro volcanic rocks, giving a minimum depth to the Precambrian basement of at least 1.5 km (5200 ft).

GEOTHERMAL RESOURCE

In the latter part of 1980 a geological reconnaissance to determine the geothermal potential of a portion of the San Pedro River valley was undertaken. The study area extends from the town of Mammoth, Pinal County, to just north of the Johnny Lyon Hills in Cochise County. In addition to a study of the pre-existing literature, a reconnaissance field study was conducted during which 16 water samples and

17 mercury soil samples, covering over 80 line km, were collected. The investigation of Hookers Hot Springs was conducted by geologist Jim Witcher as part of his study and evaluation of the warm and hot springs of Arizona.

The water-sampling program was unsatisfactory because of analytical errors in the water analyses from two different laboratories. Partial analyses are reported for these samples, four of which are duplicates (Tables 1 and 2). Current U. S. Geological Survey WATSTORE data have been used to define the chemical regime of the water. While the writer has some confidence in the results reported as partial analyses, he has elected not to combine his data with the U.S.G.S. WATSTORE data because of the element of doubt that exists with the results of his survey.

In looking at the WATSTORE data, the San Pedro area was defined by latitudes $32^{\circ}10'$ to $32^{\circ}45'$ N. and longitude $110^{\circ}10'$ to $110^{\circ}45'$ W. This area includes the far eastern portion of Tucson, the northern part of the Rincon Mountains, the eastern half of the Santa Catalina Mountains and the southern three-quarters of the Galiuro Mountains as well as the San Pedro River valley in the study area. In this large area there are 76 chemical analyses six of which are from wells in the Tucson Basin. Where there is more than one analysis for a well, the most recent analysis was used. Not all the analyses have recorded temperatures and not all are complete. However, there is more than

TABLE 1

SAN PEDRO RIVER VALLEY STUDY

Partial Chemical Analyses

Water Samples

Sample number	mg/l Ca	mg/l Mg	ppm K	ppm Li	mg/l Na	mg/l Cl	ppm B	mg/l N	mg/l CO_3	mg/l HCO_3	mg/l SO_4	mg/l F	ppm TDS	pH
Sp-1	70	11.8	3.1	0.04	39	16	0.14	4.2	0	251	42	0.77	434	7.65
Sp-2	82	15	4.0	0.06	59	16	0.19	0.5	0	307	96	1.15	575	7.60
Sp-3	95	17	4.26	0.07	64	30	0.21	0.5	0	312	132	1.15	650	7.45
Sp-4	94	13.6	3.77	0.04	52	18	0.20	0.75	0.75	273	113	1.0	564	7.60
Sp-5	66	9	4.27	0.12	46	18	0.15	0.5	0	278	72	0.9	489	7.50
Sp-6	12	0.59	2.92	0.22	98	34	0.19	0.4	4.8	117	96	4.2	362	8.2
Sp-7	13	0.58	2.78	0.22	96	34	0.19	0.4	4.8	112	98	4.22	358	8.2
Sp-8	17	0.47	1.73	0.23	128	49	0.26	0.45	3.6	105	150	4.55	453	8.1
Sp-9	4.4	0.3	1.98	0.21	71	10	0.14	0.5	9.6	146	15	3.85	256	8.5

TABLE 2

SAN PEDRO RIVER VALLEY STUDY

Partial Chemical Analyses

Water Samples

	SP-10	11	12	13	14	15	16
Lithium	0.18	0.26	0.16	0.17	0.15	0.10	<0.01
Chloride	31	35	28	31	9	11	13
Boron	<0.01	<0.01	<0.01	<0.01	<0.01	<0.01	<0.01
SiO_2	29	50	32	29	30	25	4
Sulfate	95	195	82	73	19	38	22
Fluoride	1.98	7.05	6	5	6.98	2.60	1.05
pH	7.94	7.54	8.38	8.51	8.77	7.87	7.28

nough data to characterize the water in the San Pedro iver valley.

Gradients where data were available were calculated using the following formula:

$$\text{gradient} = \frac{\text{well temperature} - \text{mean annual temperature}}{\text{depth}} \times 1000$$

The gradients are in $^{\circ}C/km$.

The Na-K-Ca geothermometers were calculated using the formula of Fournier and Truesdell (1973).

$$t^{\circ}C = \frac{1647}{\log (Na/K) + \beta \log (Ca/Na) + 2.24} - 273$$

$$\beta = 4/3 \text{ if } T < 100^{\circ}C$$

$$\beta = 1/3 \text{ if } T > 100^{\circ}C$$

The silica geothermometers were calculated according to Fournier and Rowe (1966). The chalcedony geothermometer was used because of the greater tendency for correlation with the known reservoir temperatures in southern Arizona, the Na-K-Ca geothermometer, and the geology of the area of investigation.

Both the SiO_2 and Na-K-Ca geothermometers were developed to estimate reservoir temperatures for high-temperature ($>150^{\circ}C$) geothermal resources. The geothermometers are not accurate when dealing with low- to moderate-temperature resources in a sedimentary alluvial basin. It is quite probable that numerous chemical reactions take place as the water migrates through the diverse lithologies that occur

in the basins. Hence the results of the geothermometers should only be considered a very rough approximation and may be too high or too low. Table 3 is the compilation of the results of the SiO_2 and Na-K-Ca geothermometers from the sixteen samples collected in the San Pedro River valley. The Na-K-Ca results are reported from analyses from one laboratory and the SiO_2 analyses are reported from analyses from another laboratory.

Table 4 is the chemical analyses from the WATSTORE file for wells in the area of interest. Record 61 is from one of the springs at Hookers Hot Springs. Records 43, 44, 45, 46, 64 and 65 are from the far east side of Tucson.

Table 5 is the geothermometer and geothermal gradient values calculated from the WATSTORE data. In calculating the gradient a mean annual air temperature of 18°C (Witcher, 1981) was used. Those gradients followed by an asterisk are calculated from wells less than 91.4 m (300 ft) deep. Figure 6 is a computer plot of the geothermal gradients in the San Pedro River valley and Fig. 7 is a computer contoured map of the gradients. The program for contouring averages the points in a given area. Thus there is less of a tendency for the computer to generate a series of "bulls eyes" around high points. The only real drawback to this approach is that some of the higher data points might not be reflected in the contouring if they are surrounded by lower values and are thereby averaged downward.

TABLE 3

GEOTHERMOMETERS

	Na-K-Ca		SiO_2 (Chalcedony)
SP-1	30.25°C	SP-10	46.74°C
SP-2	37.38	SP-11	72.03
SP-3	37.17	SP-12	51.03
SP-4	32.57	SP-13	46.74
SP-5	40.64	SP-14	48.20
SP-6	69.18	SP-15	40.48
SP-7	65.67	SP-16	-20.55
SP-8	49.77	SP-16	12.31 (quartz geothermometer)
SP-9	74.61		

Explanation

1. Na-K-Ca calculated with $\beta = 4/3$ and no magnesium correction was necessary.

2. Sample SP-10 is a duplicate of sample SP-8.
   Sample SP-12 is a duplicate of sample SP-7.
   Sample SP-13 is a duplicate of sample SP-6.
   Sample SP-14 is a duplicate of sample SP-9.

3. SP-16 is from a well in a small alluvial-filled valley at the west edge of the Galiuro volcanic mountains. The water comes from rain and snow melt in the Galiuro Mountains. The water is not in equilibrium with chalcedony but with quartz from volcanic rocks. The quartz geothermometer approximates the mean annual temperature at the well site.

R	LOCATION	LATITUDE	LONGITUDE	DATE	TEMP (°C)	PH	HCO3 (MG/L)	CO3 (MG/L)	CA (MG/L)	[illegible] (MG/L)	(MG/L)	(MG/L)	[illegible] (MG/L)		
8	D142122CBB	32 12.117	110 11.850	51-01-19			113.0	0.0	21.0	3.1			11.0	6.4	0.4
2	D132121ABA	32 17.733	110 12.300	78-10-03	25.0		170.0		34.0	12.0	14.0	1.6	11.0	7.5	0.6
0	D132105CDD	32 19.583	110 13.633	78-10-06	26.5										1.1
51	D132106AAC	32 20.167	110 14.300	78-10-06	39.0	8.4	130.0	17.0	1.0	0.1	66.0	0.6	3.7	4.8	2.0
77	D142119CAD	32 11.950	110 14.500	50-11-30			373.0	0.0	33.0	33.0			73.0	80.0	4.4
73	D142012CBD	32 13.650	110 15.467	65-01-01	20.0		321.0	0.0	60.0	39.0			20.0	48.0	0.7
67	D142001BBA	32 14.950	110 15.467	50-11-29			222.0	18.0					11.0		
58	D132024BDA	32 17.467	110 15.600	46-04-05			410.0	0.0	36.0	18.0			19.0	14.0	0.8
42	D122011DAD	32 24.100	110 16.150	50-11-21			251.0	17.0	40.0	29.0			5.0	16.0	0.8
63	D132209CD	32 18.800	110 16.583	51-07-12			290.0	0.0	71.0	22.0			18.0	22.0	0.4
57	D132023DCC	32 16.967	110 16.600	52-05-27	29.0		263.0	0.0	168.0	74.0			1330.0	4600.0	1.6
76	D142034CAA	32 10.283	110 17.233	78-08-10	25.0	7.4									1.3
75	D142034BBC	32 10.617	110 17.617	54-04-01	28.0		208.0	0.0	29.0	7.8			12.0	43.0	1.0
74	D142033AAD	32 10.633	110 17.750	65-05-01			228.0	0.0	43.0	17.0			14.0	102.0	
41	D122009BAA	32 24.633	110 18.717	50-11-15	17.0		303.0	0.0	62.0	24.0			7.0	23.0	0.8
72	D142008DCD	32 13.467	110 19.033	78-06-06	22.0	7.8									1.2
70	D142008BDD	32 13.900	110 19.267	78-06-06	21.0	7.6	390.0	0.0	130.0	42.0	260.0	5.4	110.0	540.0	1.3
71	D142008CBA	32 13.767	110 19.533	50-10-11	24.0		246.0	0.0	50.0	15.0			11.0	94.0	1.4
68	D142008BBD	32 14.133	110 19.533	50-10-13			270.0	0.0	58.0	19.0			20.0	136.0	1.2
59	D132032CBD	32 15.417	110 19.917	78-10-08											1.5
56	D132007DDD	32 18.683	110 20.250	53-06-02	31.0		273.0	0.0	40.0	12.0			9.0	8.4	1.0
52	D131912DCC	32 18.800	110 21.350	78-08-09		7.5	230.0	0.0	40.0	9.8	43.0	4.4	7.5	31.0	0.9
54	D131924CCC	32 17.033	110 21.850	50-10-11	22.0		298.0	0.0	53.0	22.0			17.0	137.0	1.8
50	D131910DBD	32 18.967	110 23.283	50-10-13	21.0		292.0	0.0					9.0		
36	D111910DCA	32 29.250	110 23.367	51-06-15	23.0		232.0	0.0	56.0	9.9			9.0	18.0	
51	D131910DCB	32 18.867	110 23.383	46-07-01			269.0	0.0					8.0		
66	D141927CDC	32 10.783	110 23.433	50-11-27			347.0	30.0	68.0	45.0			52.0	18.0	0.4
53	D131921BAA	32 17.800	110 24.500	78-08-10	28.0	7.6									1.0
49	D131904CDA	32 19.750	110 24.517	50-10-11	19.0		269.0	0.0					10.0		
29	D101930BDA	32 32.283	110 26.467	51-06-15			194.0	0.0	12.0	2.8			11.0	28.0	1.8
37	D111931CCD	32 25.700	110 26.833	50-11-02	21.0		145.0	0.0	30.0	9.3			7.0	22.0	0.6
9	D081813DAD	32 44.033	110 26.900	51-02-07			327.0	0.0	50.0	29.0			7.0	13.0	0.2
55	D131930CCD	32 16.167	110 26.917	78-08-11	24.0	7.8									0.4
47	D131801AAA	32 20.383	110 27.100	51-01-26	18.0		234.0	0.0	66.0	9.4			6.0	23.0	0.2
40	D121813DBC	32 23.300	110 27.483	78-06-07	20.0	7.6	200.0	0.0	80.0	19.0	57.0	4.2	18.0	200.0	0.8
39	D121813CAB	32 23.400	110 27.733	78-06-07	22.0	7.4									1.3
48	D131811AAD	32 19.400	110 28.117	51-01-26	20.0		266.0	0.0					5.0		
33	D111814CDD	32 28.250	110 28.567	78-08-16	24.0	8.0	280.0		97.0	21.0	74.0	4.1	31.0	200.0	1.1
10	D081814BCD	32 44.283	110 28.767	51-05-02	21.0		183.0	0.0	240.0	80.0			31.0	858.0	0.5
13	D081822AD	32 43.400	110 29.083	51-02-07	9.5		170.0	0.0	32.0	12.0			11.0	5.4	0.2
38	D121803AAA	32 25.583	110 29.150	62-09-16	20.0	7.4	271.0	0.0					14.0		1.1
27	D101803BAD	32 35.833	110 29.533	54-03-30	41.0		129.0	0.0	28.0	2.3			42.0	150.0	7.0
11	D081815CBA	32 44.167	110 29.700	78-06-15	28.0	7.7	180.0	0.0	34.0	5.1	24.0	0.4	7.5	4.6	0.6
8	D081810C	32 44.917	110 29.833	51-05-29	25.5		66.0	0.0	119.0	72.0			20.0	579.0	2.1
28	D101821DBA	32 32.950	110 30.267	78-06-21	20.0	9.0	290.0	0.0	95.0	19.0	62.0	4.1	12.0	190.0	1.1
12	D081817ADD	32 44.267	110 31.067	72-11-20	19.5	7.1	205.0	0.0	110.0	45.0	36.0	4.4	11.0	370.0	0.3
35	D111818BBD	32 22.950	110 33.000	78-08-14	26.0	7.2									0.3
22	D091724DDC	32 37.817	110 33.250	78-06-15	31.0	8.6	120.0	1.0	10.0	0.3	110.0	2.8	27.0	100.0	5.2

+ Hookers Hot Springs

)	LOCATION	DATE	SIO2 (MG/L)	B (µG/L)	LI (MG/L)	TDS (MG/L)	DEPTH (FEET)	ID
8	D142122CB3	51-01-19	12.0			130.0	705.0	
2	D132121A9A	78-10-03	34.0	30.0		208.0		
0	D132105CDD	78-10-06						
1	D132106AAC	78-10-06	46.0	70.0		207.0		
7	D142119CAD	50-11-30	22.0			562.0	644.0	
3	D142012C9D	55-01-01	24.0			376.0	12.0	
7	D142001B3A	50-11-29						
8	D132024BDA	46-04-05				390.0	38.0	
2	D122011OAD	50-11-21	78.0			329.0	312.0	
3	D132209CD	51-07-12	53.0			364.0		
57	D132023DCC	52-05-27	28.0			9160.0		
76	D142034CAA	78-08-10					145.0	
75	D142034B3C	54-04-01	29.0			286.0	246.0	
74	D142033AAD	55-05-01				466.0		
41	D122009BAA	50-11-15	69.0			355.0	25.0	
72	D142008DCD	78-06-06						
70	D142008BDD	78-06-06	31.0	570.0		1330.0		
71	D142008C3A	50-10-11	32.0			386.0	125.0	
68	D142008B8D	50-10-13	32.0			484.0	60.0	
59	D132032CBD	78-10-08						
56	D132007DDD	53-06-02	37.0				440.0	
52	D131912DCC	78-08-09	45.0	50.0		300.0		
54	D131924CCC	50-10-11	31.0			499.0	70.0	
50	D131910BBD	50-10-13					27.0	
36	D111910DCA	51-06-15				226.0	300.0	
51	D131910DC8	46-07-01					102.0	
66	D141927CDC	50-11-27	33.0			451.0	20.0	
53	D131921BAA	78-08-10						
49	D131904C9A	50-10-11					133.0	
29	D101930BDA	51-06-15	44.0				490.0	
37	D111931CCD	50-11-02	45.0			214.0		
9	D081813DAD	51-02-07	55.0			343.0		
55	D131930CCD	78-08-11						
47	D131801AAA	51-01-26	19.0				180.0	
40	D121813D9C	78-06-07	27.0	90.0		530.0		
39	D121813CAB	78-06-07						
48	D131811AAD	51-01-26					220.0	
33	D111814CDD	78-08-16	37.0	80.0		637.0		
10	D081814BCD	51-05-02	32.0			1410.0		
13	D081822AD	51-02-07	57.0			218.0		
38	D121803AAA	52-09-16					122.0	
27	D101803BAD	54-03-30	41.0				277.0	
11	D081815C8A	78-06-15	53.0	20.0		220.0		
8	D081810C	51-05-29	32.0			902.0		
28	D101821D9A	78-06-21	29.0	110.0		564.0		
12	D081817ADD	72-11-20	33.0	30.0		720.0		
35	D111818B3D	78-08-14						
22	D091724DDC	73-06-15	35.0	140.0		352.0		

+ Hookers Hot Springs

SAN PEDRO - Table 4

D R	LOCATION	LATITUDE	LONGITUDE	DATE	TEMP (°C)	PH	HCO3 (MG/L)	CO3 (MG/L)	CA (MG/L)	MG (MG/L)	NA (MG/L)	K (MG/L)	CL (MG/L)	SO4 (MG/L)	F (MG/L)
6	D081736ACD	32 41.683	110 33.367	54-11-13		9.5	96.0	47.0	0.8	0.2			6.0	7.6	30.0
7	D081732DAA	32 37.917	110 33.467	80-11-28	32.0	8.5			7.6	0.3	110.0	3.6	28.0	100.0	5.7
23	D091725DBB	32 37.117	110 33.500	54-10-09	22.0		162.0	0.0	13.0	2.9			7.0	17.0	1.4
31	D111724CAC	32 27.750	110 33.983	52-07-08	27.0		188.0	0.0	45.0	11.0			4.0	15.0	0.4
21	D091723DDD	32 37.800	110 34.167	54-10-09	23.0		184.0	0.0	15.0	0.9			8.0	34.0	2.2
19	D091714CDD	32 38.667	110 34.617	50-09-28	31.0		173.0	0.0	5.5	0.9			7.0	20.0	2.8
17	D091714CDB	32 38.783	110 34.750	50-09-28	31.0		176.0	0.0	48.0	4.9		44.0		212.0	6.0
18	D091714CDC	32 38.667	110 34.767	78-06-14	23.0	7.5									4.2
26	D101727DCA	32 31.900	110 35.483	49-08-12			117.0	0.0	21.0	9.7			6.0	14.0	0.2
20	D091722ABB	32 38.517	110 35.500	54-03-24	28.0		178.0	0.0					10.0		
16	D091710DCB	32 39.633	110 35.550	50-09-28	32.0		235.0						42.0		
25	D101715BBB	32 34.217	110 36.067	51-06-15	22.0		235.0	0.0	42.0	16.0			10.0	6.0	0.4
4	D081729DDA	32 42.200	110 37.250	78-06-14	23.0	7.7									3.5
5	D081732DAA	32 41.600	110 37.267	78-06-14	41.0	8.6	110.0	0.0	0.4	4.0	130.0	1.8	42.0	150.0	6.1
24	D101705BCA	32 35.783	110 38.033	54-03-24	26.0		228.0	0.0	46.0	12.0			21.0	4.5	0.8
3	D081719DAD	32 43.200	110 38.267	63-09-11		7.0	245.0	0.0					38.0		3.1
32	D111730AAA	32 27.367	110 38.400	52-07-10	21.0		327.0	0.0	90.0	14.0			4.0	15.0	0.1
30	D111718ACA	32 28.850	110 38.517	78-08-15			210.0		64.0	10.0	9.2	3.0	6.2	48.0	0.4
* 43	D131601CC	32 19.783	110 40.400	52-11-13			170.0	6.0	36.0	6.6			8.0	4.5	1.4
14	D091602BAB	32 41.150	110 40.950	51-05-29	38.0		349.0	0.0	69.0	21.0			32.0	39.0	2.6
* 64	D141603DBB	32 14.450	110 41.617	68-04-09		7.5	90.0	0.0	25.0	3.2			13.0	60.0	1.4
* 65	D141609AAB	32 14.067	110 42.367	62-03-10			78.0	0.0	28.0	6.0			12.0	16.0	0.4
15	D091609BDB	32 40.150	110 42.983	78-08-31	28.0	7.5	310.0		52.0	22.0	36.0	4.1	21.0	17.0	0.9
* 46	D131620DDD	32 16.817	110 43.333	66-11-12		8.4	222.0	6.0	56.0	24.0			58.0	172.0	4.2
2	D081620ADA	32 43.517	110 43.333	78-08-31	27.0	7.7									2.9
* 45	D131620DC	32 16.867	110 43.800	42-02-05	30.0		205.0	0.0	32.0	6.1			30.0	176.0	6.5
1	D081618DDC	32 43.867	110 44.500	78-08-31		7.7									1.5
* 44	D131619CAD	32 17.050	110 44.817	58-05-09			63.0	0.0	316.0	5.0			150.0	3680.0	0.0

otal number of records: 76.
LL
4-FEB-81

* Tucson wells

	LOCATION	DATE	SIO2 (MG/L)	B (UG/L)	LI (MG/L)	TDS (MG/L)	DEPTH (FEET)
	D081736ACD	54-11-13	55.0				425.0
7	D081732DAA	80-11-28	36.0	90.0	200.0	351.0	
3	D091725DBB	54-10-09	37.0				1006.0
1	D111724CAC	52-07-08	26.0				160.0
1	D091723DDD	54-10-09	33.0				1005.0
9	D091714CDD	50-09-28	35.0				
7	D091714CDB	50-09-28	47.0				54.0
8	D091714CDC	78-06-14					
6	D101727DCA	49-08-12	36.0				462.0
0	D091722ABB	54-03-24					1107.0
16	D091710DCB	50-09-28					85.0
25	D101715BBB	51-06-15	28.0				285.0
4	D081729DDA	78-06-14					
5	D081732DAA	78-06-14	34.0	190.0		434.0	
24	D101705BCA	54-03-24	28.0				700.0
3	D081719DAD	63-09-11					46.0
32	D111730AAA	52-07-10	11.0				
30	D111718ACA	78-08-15	19.0	30.0		268.0	
43	D131601CC	52-11-13				237.0	
14	D091602BAB	51-05-29	31.0				1300.0
*64	D141603DBB	68-04-09	28.0			213.0	
*65	D141609AAB	62-03-10				141.0	
15	D091609BDB	78-08-31	25.0	100.0		348.0	
*46	D131620DDD	66-11-12	25.0			558.0	200.0
2	D081620ADA	78-08-31					
*45	D131620DC	42-02-05				493.0	
1	D081618DDC	78-08-31					
*44	D131619CAD	58-05-09				5693.0	110.0

tal number of records: 76.
L
-FEB-81

* Tucson wells

PEDRO - Table 5 04-MAR-81 11:19:28

GEOTHERMOMETER VALUES

ER	NA-K-CA (°C)	SIO2 (°C)	GRADIENT (GMAT= 18.00000) (°C/KM)
78	-------	12.66	-------
52	18.24	53.59	-------
50	-------	-------	-------
51	85.50	64.66	-------
77	-------	35.13	-------
73	-------	38.65	546.81*
67	-------	-------	-------
58	-------	-------	-------
42	-------	95.70	-------
63	-------	74.83	-------
57	-------	45.09	-------
76	-------	-------	158.39*
75	-------	46.59	133.37*
74	-------	-------	-------
41	-------	88.81	-131.23*
72	-------	-------	-------
70	50.47	49.18	-------
71	-------	50.38	157.48*
68	-------	50.88	-------
69	-------	-------	-------
56	-------	57.43	96.93
52	49.95	66.68	-------
54	-------	49.49	187.48*
50	-------	-------	364.54*
36	-------	-------	54.68*
51	-------	-------	-------
66	-------	52.25	-------
53	-------	-------	-------
49	-------	-------	24.67*
29	-------	65.59	-------
37	-------	66.68	-------
9	-------	77.65	-------
55	-------	-------	-------
47	-------	29.38	0.00*
40	38.32	43.25	-------
39	-------	-------	-------
48	-------	-------	29.83*
33	37.25	56.56	-------
10	-------	50.89	-------
13	-------	78.57	-------
38	-------	-------	53.78*
27	-------	62.22	272.42*
11	75.00	74.31	-------
8	-------	50.83	-------
28	36.11	45.84	-------
12	30.34	58.56	-------
35	-------	-------	-------
22	73.12	50.30	-------
6	-------	76.72	-------
7	27.41	52.94	-------
23	-------	57.43	13.05
31	-------	41.96	134.55*
21	-------	52.25	14.32
19	-------	54.39	-------

+ Hookers Hot Springs

GEOTHERMOMETER VALUES

IBER	NA-K-CA (°C)	SIO2 (°C)	GRADIENT (GMAT= 18.00000) (°C/KM)
17	-------	68.81	789.83*
18	-------	-------	-------
26	-------	56.17	-------
20	-------	-------	29.64
16	-------	-------	540.37*
25	-------	45.09	46.05*
4	-------	-------	-------
5	139.49	43.85	-------
24	-------	45.09	37.50
3	-------	-------	-------
32	-------	9.70	-------
30	19.75	29.38	-------
* 43	-------	-------	-------
14	-------	49.49	50.47
* 54	-------	45.09	-------
* 65	-------	-------	-------
15	41.77	40.07	-------
* 46	-------	40.33	-------
2	-------	-------	-------
* 45	-------	-------	-------
1	-------	-------	-------
* 44	-------	-------	-------

* Tucson wells

In Fig. 6, to avoid crowding, the computer was programmed not to print the value at any point that is within 3/4 of an inch of a previously printed point. Hence some of the high gradients from Table 5 do not appear in Fig. 6 but are reflected in the contours of Fig. 7. Conversely, when the discharge temperature is less than the mean annual temperature, the computer will compute a negative gradient and contour it.

In Fig. 7 the 789+$^{\circ}$C/km is reflected in the 400 and 500°C/km contour lines near the town of San Manuel. This very high anomaly is caused by a well with a surface discharge temperature of 31°C and a depth of 16.5 m (54 ft). These gradient anomalies must not be taken literally as these high gradients do not hold at depth. Instead, they merely reflect the presence of warm water at a shallow depth. A more accurate calculated gradient for this area might be obtained from SP-10, which has a measured temperature of 40°C and a depth of 452.6 m (1485 ft). SP-10 has a calculated gradient of 48.6°C/km and is in the same cluster of wells along the San Pedro River just east of San Manuel. Table 6 is a compilation of the well gradients in the study area. Wells over 200 m in depth give a more accurate estimation of the gradient in that area. The very shallow wells, with a lightly higher discharge temperature than the mean annual air temperature, give erroneously high gradients. In all probability, the thermal gradient in the

TABLE 6

CALCULATED GRADIENTS

OF

SAMPLED WELLS

Sample No.	Discharge Temperature	Depth	Gradient
SP-1	18°C	30.48 m	0
SP-2	20°C	30.48 m	65.61°C/km
SP-3	20°C	33.53 m	59.65°C/km
SP-4	20°C	30.48 m	65.61°C/km
SP-5	20°C	18.29 m	109.36°C/km
SP-10	40°C	452.60 m	48.60°C/km
SP-11*	31°C	30.48 m	426.51°C/km
SP-12	31°C	265.18 m	49.02°C/km
SP-13	30°C	251.46 m	47.72°C/km
SP-14	30°C	259.08 m	46.32°C/km
SP-15+	23.5°C	294.74 m	18.66°C/km
SP-16	21°C	depth not available	

Calculated with a mean annual air temperature of 18°C

*SP-11 is within 100 feet of SP-12 which is now abandoned and its casing is in deplorable condition. It would be reasonable to assume lateral migration of warm water through rusted out casing into the production zone of SP-11.

+SP-15 is Well #2 at Magma Copper Company. The well is reported "hot" artesian well by the U.S. Geological Survey on the Peppersauce Wash 7½ minute topographic quadrangle, Section 25, T. 9 S., R. 17 E. On tables 4 and 5 record number 23 is another Magma Copper Company well in the same section with a measured temperature of 22°C, a depth of 306.6 m, and a gradient of 13.05°C/km. These very low gradients do not approximate the average gradient for the Basin and Range province of 30°C/km. These wells are part of the well field that supplies water to the Magma mill and smelter. The only explanation for these anomalously low gradients is that the wells for one reason or another are no longer producing from the horizon in which they bottomed or from which they originally produced.

San Manuel area of the San Pedro River valley is 47 or 48°C/km.

Similarly in the southeast corner of Fig. 6, the gradient 546.8°C/km, well record 73, is generated by a well with a measured temperature of 20°C, two degrees above mean annual air temperature, and a depth of 3.67 m (12 ft). This extremely high gradient again points out the problem of using gradients from shallow wells. Calculated gradients, assuming no infusion of cold water up hole, assume a degree of reliability when the depth of the well is 300 m (1000 ft) or greater. Measured gradients in water wells over 100 m (328 ft) deep have proved to be the most accurate means of establishing a geothermal gradient.

Figure 8 is a computer plot of the SiO_2 geothermometers. The geothermometers were calculated for equilibrium with chalcedony. The SiO_2 geothermometers reflect a low- to moderate-temperature geothermal resource possibly at a depth of 1 km or less.

Figure 9 is a computer generated contour map of the SiO_2 data shown in Fig. 8. The 90°C contour reflects Hookers Hot Springs. The contour map appears to indicate an overall increase in geothermometer temperatures from west to east. However, there is no available data in the Galiuro Mountains. Again, it should be pointed out that the SiO_2 and Na-K-Ca geothermometers were developed to predict high temperature, >150°C, geothermal resources, not

low- to moderate-temperature resources. Therefore, with the possible exception of Hookers Hot Springs, the geothermometers may indicate only that the water in the basin alluvial fill has had more time to dissolve silica or has been in contact with a more soluble form of silica.

Figure 10 is a plot of the available Na-K-Ca geothermometers from the WATSTORE files. Because of the paucity of points the data were not contoured. Again great caution should be taken in the interpretation of this geothermometer.

Figure 11 shows the SiO_2 geothermometer versus measured temperature. The warmer wells appear to have a maximum "reservoir(?)" temperature between 45 and 65°C assuming reliability of the geothermometer. The highest geothermometer, ≈ 90°C, and the lowest geothermometer, ≈ 10°C, come from wells with discharge temperatures approximating the mean annual temperature for the region. These results may indicate the presence of silica that is not totally dependent upon temperature for its solubility.

Hookers Hot Springs, a former spa, is located in Cochise County, Arizona, at the Muleshoe Ranch, Section 6, T. 13 S., R. 21 E. Table 7 is the chemical data from Hookers Hot Springs and springs in the immediate vicinity. The geothermometer temperatures for the different springs vary from 118-134°C for Na-K-Ca and from 95-105°C for SiO_2 (quartz conductive). Therefore, the minimum reservoir temperature for this hot spring system might be expected to be

HOOKERS HOT SPRINGS*

Sample #	Name	Township location	Sample date	Temp.	Flow (est.)	Field pH	Na	K	Ca	Mg
3W80	Hookers hot springs	T13S, R21E, Sec. 6 NE¼, NE¼, SW¼, SW¼	4/15/80	52.0°C	10 gpm	9.21	28.6	0.79	0.23	0.05
4W80	Hookers hot springs	T13S, R21E, Sec. 6 NE¼, NW¼, SE¼, NE¼	4/15/80	51.0°C	5 gpm	9.22	31.6	0.76	0.25	0.06
5W80	Hookers hot springs	T13S, R21E, Sec. 6 NE¼, NW¼, SE¼, SW¼	4/15/80	40.0°C	5 gpm	9.22	31.0	0.74	0.20	0.02
6W80	"cold" spring	T12S, R21E, Sec. 31 NE¼, NW¼, SE¼, SW¼	4/16/80	18.0°C	1 gpm	7.15	66.0	1.39	1.83	4.80
7W80	"warm" spring	T12S, R21E, Sec. 31 NE¼, SW¼, SE¼	4/16/80	29.0°C	<2 gpm	9.05	26.9	0.54	0.35	0.12
8W80	"warm" spring	T12S, R21E, Sec. 31 NE¼, SW¼, SE¼	4/16/80	32.5°C	~2 gpm	9.15	28.1	0.52	0.31	0.05

* All data from J.C. Witcher, Arizona Hot Springs Study

100°C, indicative of a low- to moderate-temperature resource. Both the writer and Witcher (pers. commun., 1980) infer that Hookers Hot Springs is structurally controlled. The exact structural details have not as yet been resolved.

Figure 12 is a plot of the measured temperatures recorded in the WATSTORE file. Hookers Hot Springs has been indicated on the map. The 39°C temperature recorded in Table 4 is from one of the lesser springs. The temperatures of the main springs at Hookers Hot Springs are in excess of 50°C.

The only other thermal well found during this study is on the property of A. C. Gruwell. This well is situated in the NW¼, SE¼, NW¼, Section 3, T10S, R18E and is erroneously reported in the WATSTORE file, record 27, as SE¼, NE¼, NW¼, Section 3, T10S, R18E. At the scale of the maps and plots in this report this quarter mile discrepancy makes no difference. This well has a measured temperature of 41°C, a depth of 84.4 m (277 ft) and a calculated gradient of 272.5°C/km, which is excessive. The well is situated in Cienega Wash and is collared in the Quiburus Formation. A possible explanation for this well, which is west of the Galiuro Mountains and reported to be artesian, rising to within 50 ft of the surface (Gruwell, pers. commun., 1981), is warm water rising along a fault, possibly one of the basin bounding faults, and then moving laterally to-

wards the center of the valley through an aquifer in the Quiburus Formation.

Figure 13 is a computer contour map of the measured temperature data. Again, the higher points are averaged with the lower points but the anomalous areas are still reflected in the map. It is interesting to note that in the northwest corner of the map the warm temperature of the water (38°C at 396 m) from a mine shaft at San Manuel indicates another anomalous area.

Figures 14 and 15 are a plot and contour map respectively of the total dissolved solids (TDS) in the study area. With the exception of one well in the Tucson (southwest corner of maps) area and three wells in the southeast corner of the map, all the reported TDS analyses are less than 1000 milligrams per liter (mg/l). The water quality in the San Pedro Valley with respect to TDS is very good, generally less than 500 mg/l. The high TDS in the southeast corner of the map is not the result of Hookers Hot Springs, which has a TDS of less than 500 mg/l. Instead, it apparently reflects local sediment conditions in the Teran basin where the middle lithologic unit composed of sandstone, shale and mudstone contains gypsiferous mudstone (Scarborough and Wilt, 1979).

In an attempt to define the water of the San Pedro Valley two triangular diagrams and five x-y plots were

generated. Geothermal waters will often have excessive concentrations of boron, fluorine, chlorine and sulfate. Comparisons of these elements and compounds will often designate different waters and mix waters in the same geographical area as well as indicate geothermal water.

The first triangular diagram (Fig. 16) is a plot of Ca-Mg-Na. Where complete analyses are available the water is primarily a calcium-sodium (Ca-Na) water low in magnesium (Mg). Those analyses where sodium (Na) is the dominate cation appear to be from the Teran basin.

The second triangular diagram (Fig. 17) is a plot of HCO_3-SO_4-Cl. Where complete analyses are available the water is primarily a bicarbonate (HCO_3) water. Those analyses where sulfate (SO_4) is the dominate anion are from the Teran basin where there is gypsum in the mudstone beds.

From the two triangular diagrams the water in the San Pedro Valley study area may be classified as a calcium-sodium bicarbonate water. This type of water appears, from prior work in Arizona, to be one of the more common types of ground water in the Basin and Range province of the state.

Figure 18 shows a comparison of the SiO_2 versus the Na-K-Ca geothermometer temperatures. There appears to be reasonable correlation between the geothermometers, given the inadequacies of the geothermometers applied to low-

temperature resources. The point at the far right of the diagram indicating reservoir temperatures of 139.40 (Na-K-Ca) and 48.85 (SiO_2) is well record 5, which is also SP-10. This warm artesian well was drilled in 1937 as an oil test. The well bottomed at approximately 453 m (1485 ft) in what is apparently Quiburus Formation. The original flow was estimated to be 20 gallons per minute from a 29 m (95 ft) thick sandstone at a depth of 1275-1370 ft (Roeske and Werrell, 1973). The writer, during this study, measured a temperature of 40°C and estimated the flow at 5 gallons per minute. In all probability the casing has deteriorated, permitting the influx up hole of sediments and cooler water. Again, great care should be taken in using the geothermometers on low- to moderate-temperature resources. Too many unknown chemical reactions can take place as the ground water migrates through the diverse lithologies of the basins.

Figures 19 and 20, computer plots of chlorine versus measured temperature and boron versus measured temperature, indicate that the presence of these two elements are not temperature dependent but are apparently dependent upon lithology.

Figure 21 is a computer plot of chlorine versus fluorine. There is no apparent relationship between the concentration of chlorine and fluorine in the water.

In an attempt to further delineate the structural geology and possible thermal areas, 80 km of reconnaissance mercury geochemical soil lines were run across the San Pedro Valley. These lines were situated perpendicular to the strike of the valley in an attempt to sample mercury vapor leaking upwards through the basin-fill material along buried fault zones. Also mercury anomalies are often associated with geothermal anomalies of igneous origin (Matlick, 1975). Figure 22 shows the location of the soil-sample lines and the values in parts per billion (ppb) mercury (Hg). Table 8 lists the values for the mercury samples. A background value of 65 ppb Hg was determined by statistics. The writer considers values 2½ times background or greater to be anomalous. SP-36 (160 ppb Hg) is the only anomalous value. This sample was taken in the proximity of weakly mineralized outcrops of Precambrian and Paleozoic sediments.

It may be concluded from the results of the mercury sampling program that no fault structures were delineated by anomalous mercury values. Possibly the faults along the sample lines were cemented closed by minerals precipitating from ground water or possibly there is an impermeable barrier in the basin fill material that is blocking the upward movement of mercury vapor or maybe there is no Hg vapor.

TABLE 8

MERCURY GEOCHEMISTRY SOIL SAMPLES

Sample Number	Hg ppb	Sample Number	Hg ppb	Sample Number	Hg ppb
SP-1	65	SP-18	65	SP-35	40
SP-2	40	SP-19	55	SP-36	160
SP-3	45	SP-20	95	SP-37	65
SP-4	85	SP-21	65	SP-38	40
SP-5	55	SP-22	55	SP-39	40
SP-6	75	SP-23	105	SP-40	60
SP-7	105	SP-24	65	SP-41	65
SP-8	40	SP-25	65	SP-42	65
SP-9	45	SP-26	85	SP-43	65
SP-10	85	SP-27	75	SP-44	95
SP-11	85	SP-28	55	SP-45	80
SP-12	65	SP-29	30	SP-46	95
SP-13	65	SP-30	75	SP-47	85
SP-14	65	SP-31	20	SP-48	45
SP-15	65	SP-32	45	SP-49	45
SP-16	85	SP-33	45	SP-50	30
SP-17	65	SP-34	30		

Sample number with mercury values in parts per billion

CONCLUSIONS

Three anomalous areas containing shallow-depth warm water have been located in the San Pedro study area: (1) the San Manuel-Mammoth area; (2) the A.C. Gruwell Ranch; (3) Hookers Hot Springs at the Muleshoe Ranch.

The probable explanation for these warm water resources is as follows.

The Galiuro Mountains, the remains of a volcanic pile deposited along the axis of a large synform (Rehrig and Heidrick, 1976), are in all probability an area of recharge for the ground water system in the area. The meteoric water falling down upon the Galiuro Mountains percolates downward to great depths through fractures in the volcanic rocks, becomes heated, rises by convection along faults, encounters late Tertiary sedimentary units overlying these faults and migrates laterally through these sediments out into the basin. These warm waters are now near the surface because of erosion of the late Tertiary and Quaternary sedimentary units by the San Pedro River. This type of phenomenon will readily explain the unreasonably high gradients encountered in some of the more shallow wells.

This low- to moderate-temperature geothermal resource may be utilized using current heat-pump technology for space heating and cooling, green house operations or in health spas. However, the size and production capabilities of the reservoir(s) has yet to be established.

REFERENCES

Chapin, E.E., Chamberlin, R.M., Osburn, G.R. and White, D.W., 1978, Exploration framework of the Socorro geothermal area, New Mexico, in Chapen, C.E. and Elston, W.E., Special publication, New Mexico Geological Society, p. 115-129.

Cooper, J.R., 1959, Some geologic features of the Dragoon quadrangle, Arizona, in Heindl, L.A., ed., Southern Arizona Guidebook II, Arizona Geological Society, p. 139-145.

Drewes, H. and Thorman, C.H., 1978, Major geologic structures between Lordsburg, New Mexico and Douglas and Tucson, Arizona, in Callender, J.F., Wilt, J.C. and Clemons, R.E., eds., Land of Cochise, Southeastern Arizona; New Mexico Geological Society, Twenty-ninth Field Conference, p. 291-295.

Durning, W.P. and Davis, J.D., 1978, The root-zone characteristics of porphyry copper deposits, in Proceedings of the Porphyry Copper Symposium, Arizona Geological Society Digest, v. 12, p. 81-89.

Fenneman, N.M., 1931, Physiography of western United States: McGraw-Hill Book Company, Inc., p. 326-395.

Fournier, R.O. and Rowe, J.J., 1966, Estimation of underground temperatures from silica content of water from hot springs and wet steam wells: American Journal of Science, v. 264, p. 685-697.

Fournier, R.O. and Truesdell, A.H., 1973, An empirical Na-K-Ca geothermometer for natural waters: Geochemica et Cosmochemica Acta, v. 37, p. 1255-1275.

Gruwell, A.C., 1981, personal communication.

Heindl, L.A., 1963, Cenozoic geology in the Mammoth area, Pinal County, Arizona: U.S.G.S. Bulletin, 1141-E, p. 41.

Krieger, M.H., 1974, Generalized geology and structure of the Winkelman 15-minute quadrangle and vicinity, Pinal and Gila counties, Arizona: U.S.G.S. Journal of Research, v. 2, no. 3, p. 311-321.

Krieger, M.H., Cornwall, H.R. and Banks, N.G., 1974, The Big Dome Formation and revised Tertiary stratigraphy in the Ray-San Manuel area, Arizona: U.S.G.S. Bulletin 1394-A, p. 54-62.

Lysonski, J.C., Aiken, C.L.V. and Sumner, J.S., 1981, Complete residual Bouguer gravity anomaly map, Tucson; scale 1:250,000, Bureau of Geology and Mineral Technology, open file.

Matlick, J.S., III, 1975, A new geothermal exploration method using mercury: Unpublished M.S. thesis, Arizona State University, 83 p.

Menges, C., 1981, personal communication.

Montgomery, E.L., 1963, The geology and ground water investigation of the Tres Alamos dam site area of the San Pedro River, Cochise County, Arizona: M.S. thesis, University of Arizona, 61 p.

Rehrig, W.A. and Heidrick, T.L., 1976, Regional tectonic stress during Laramide and late Tertiary intrusive periods, Basin and Range province, Arizona, in Wilt, J.C. and Jenney, J.P., eds., Tectonic Digest, Arizona Geological Society Digest, v. X, p. 205-228.

Roeske, R.H. and Werrell, W.L., 1973, Hydrologic conditions in the San Pedro River valley, Arizona, 1971: Arizona Water Commission, Bulletin 4, Phoenix, 76 p.

Sauck, W.A. and Sumner, J.S., 1971, Residual aeromagnetic map of Arizona; scale 1:250,000, University of Arizona Press.

Scarborough, R.B., 1975, Chemistry and age of late Cenozoic air-fall ash in southeastern Arizona: Unpublished M.S. thesis, University of Arizona, 107 p.

Scarborough, R.B. and Wilt, J.C., 1979, A study of uranium favorability of Cenozoic sedimentary rocks, Basin and Range province, Arizona, Part I: Bureau of Geology and Mineral Technology, Geological Survey Branch, Tucson, 101 p.

Schmitt, H.A., 1966, The porphyry copper deposits in their regional setting, in Titley, S.R. and Hicks, C.L., eds., Geology of the Porphyry Copper Deposits Southwestern North America, University of Arizona Press, p. 17-34.

Silver, L.T., 1978, Precambrian formations and Precambrian history in Cochise County, southeastern Arizona, in Callender, J.F., Wilt, J.C., and Clemons, R.E., eds., Land of Cochise, Southeastern Arizona; New Mexico Geological Society, Twenty-ninth Field Conference, p. 157-163.

Swan, M.M., 1976, The Stockton Pass fault: an element of the Texas lineament: Unpublished M.S. thesis, University of Arizona, 119 p.

Titley, S.R., 1976, Evidence for a Mesozoic linear tectonic pattern in southeastern Arizona, in Wilt, J.C. and Jenney, J.P., eds., Tectonic Digest, Arizona Geological Society Digest, v. X, p. 71-102.

WATSTORE, 1981, U.S. Geological Survey.

Witcher, J.C., 1981, personal communication.

Witcher, J.C., 1981, Geothermal potential of the lower San Francisco River system: Bureau of Geology and Mineral Technology, Tucson, in press.

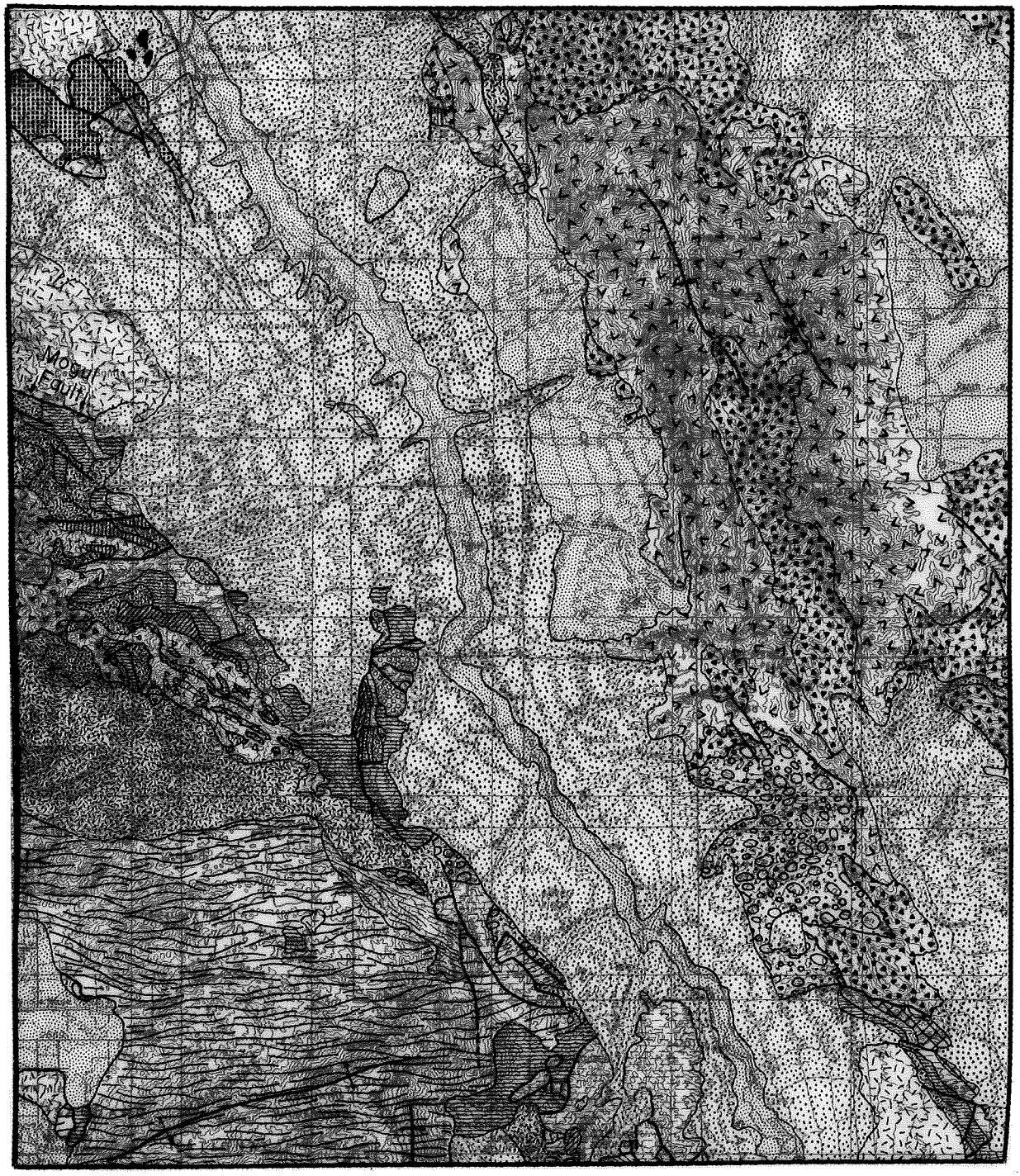

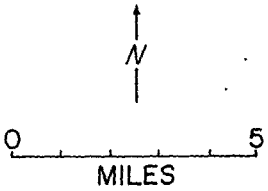

SAN PEDRO
GENERAL GEOLOGY

FROM: Wilson, Moore, and Cooper, 1969.
BASE: U.S.G.S. TUCSON 1:250,000

Figure 1

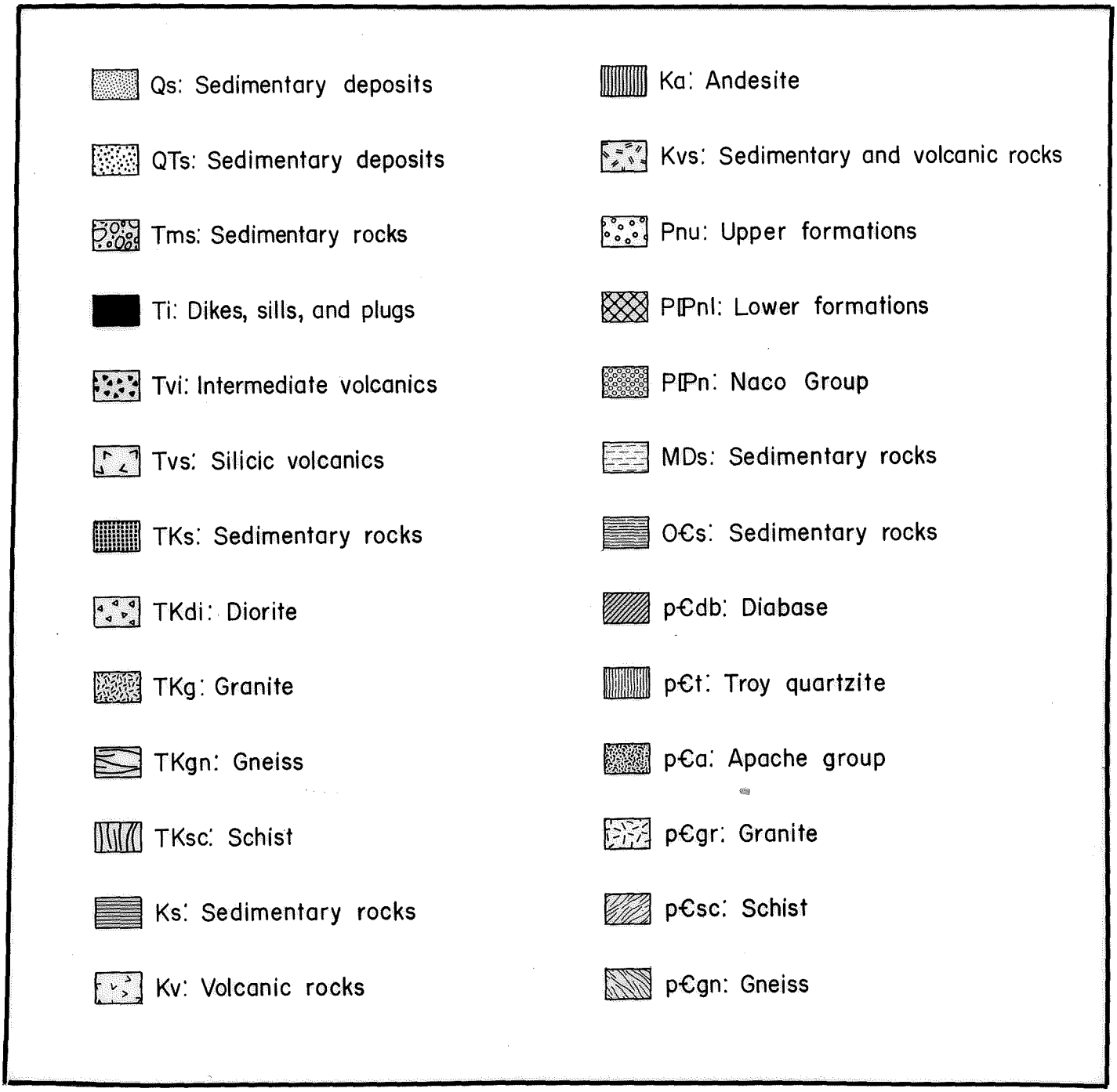

Explanation for Figure 1.

Figure 2

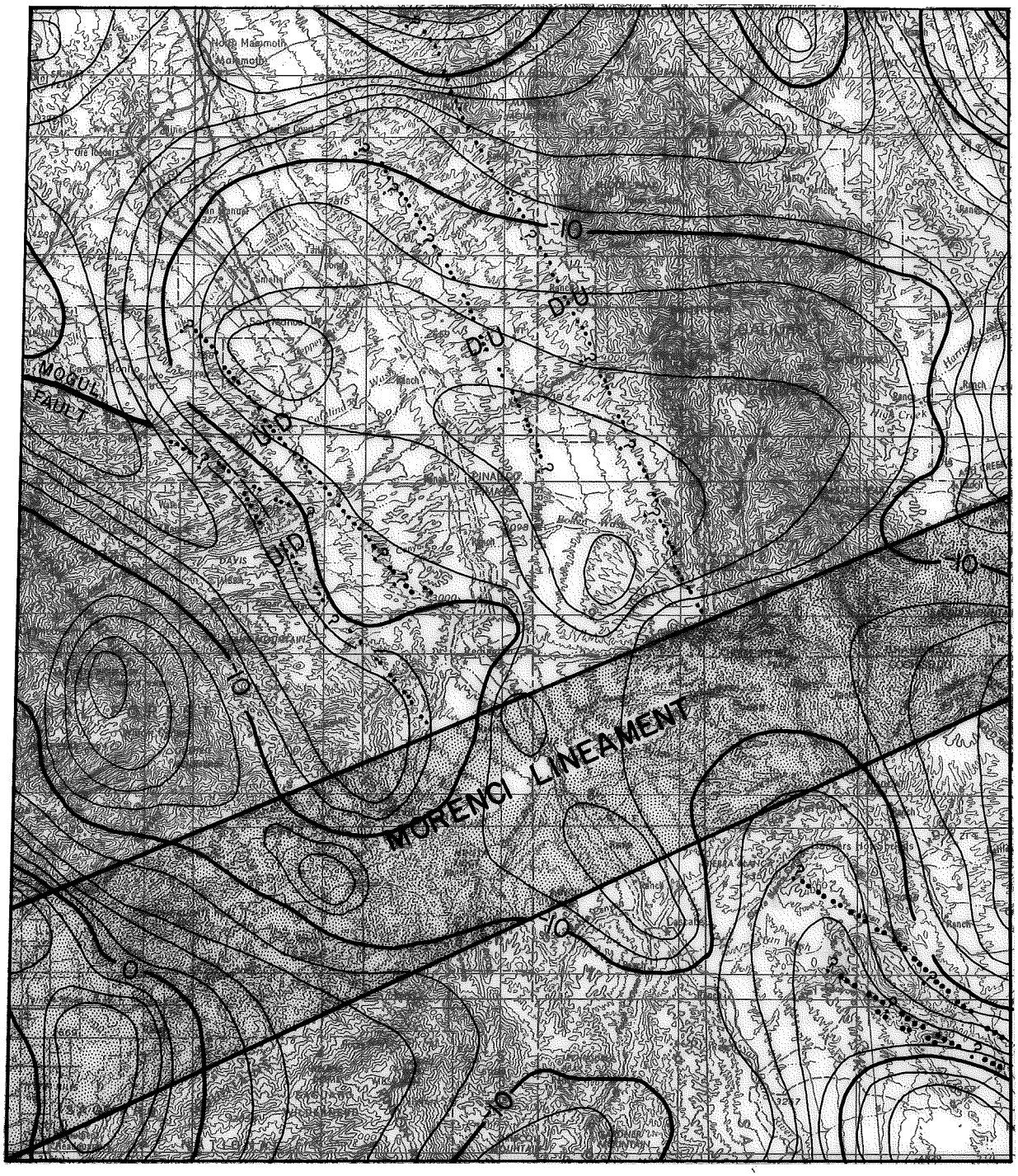

N

0 5 MILES
0 5 KILOMETERS

BASE MAP: U.S.G.S. TUCSON 1:250,000

?.....? POSTULATED AND INFERRED FAULTS

Bouguer Gravity
10 mgal contour
2 mgal contour

Figure 5

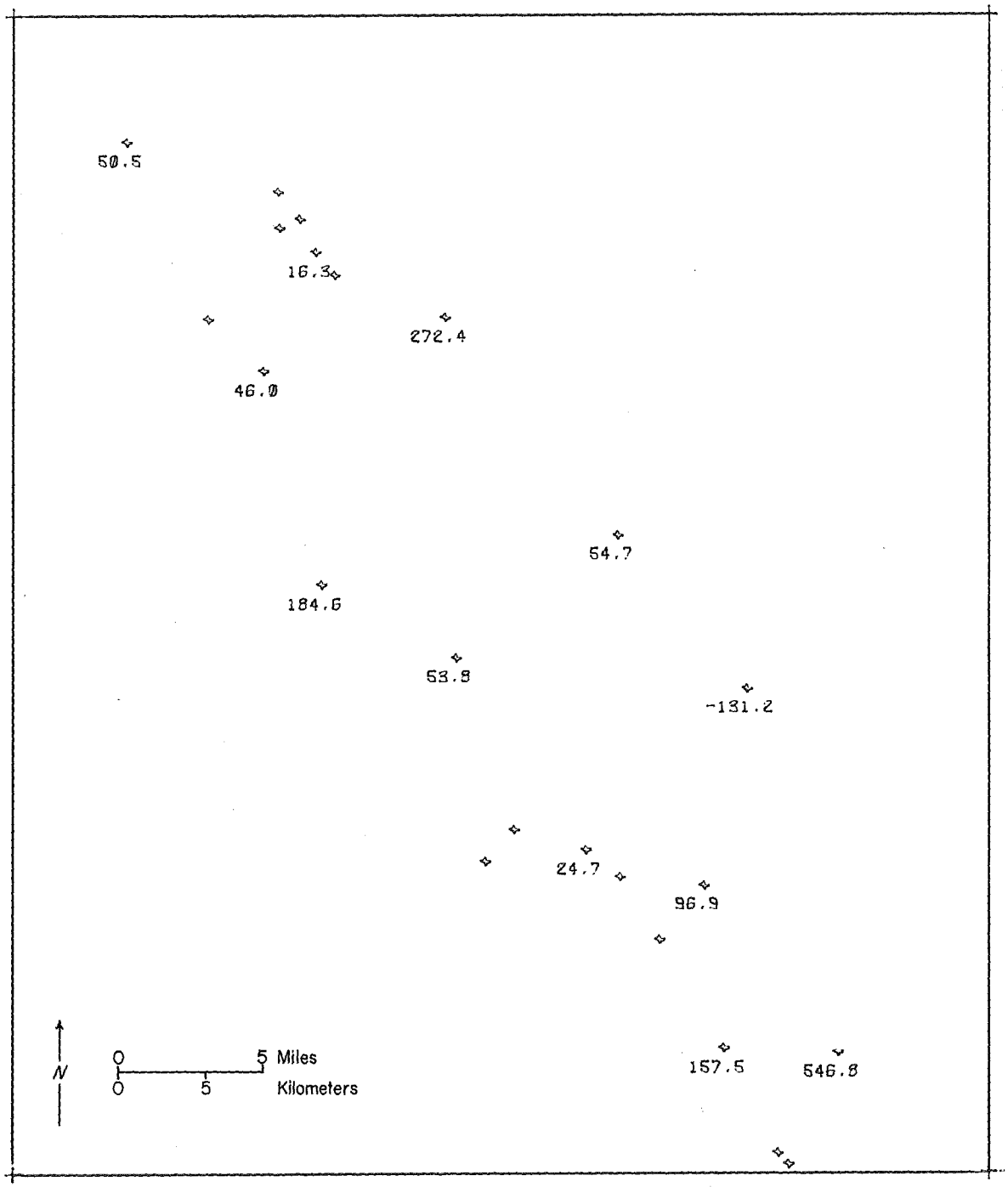

Figure 6. San Pedro geothermal gradients; gradients have been calculated in $^{o}C/km$.

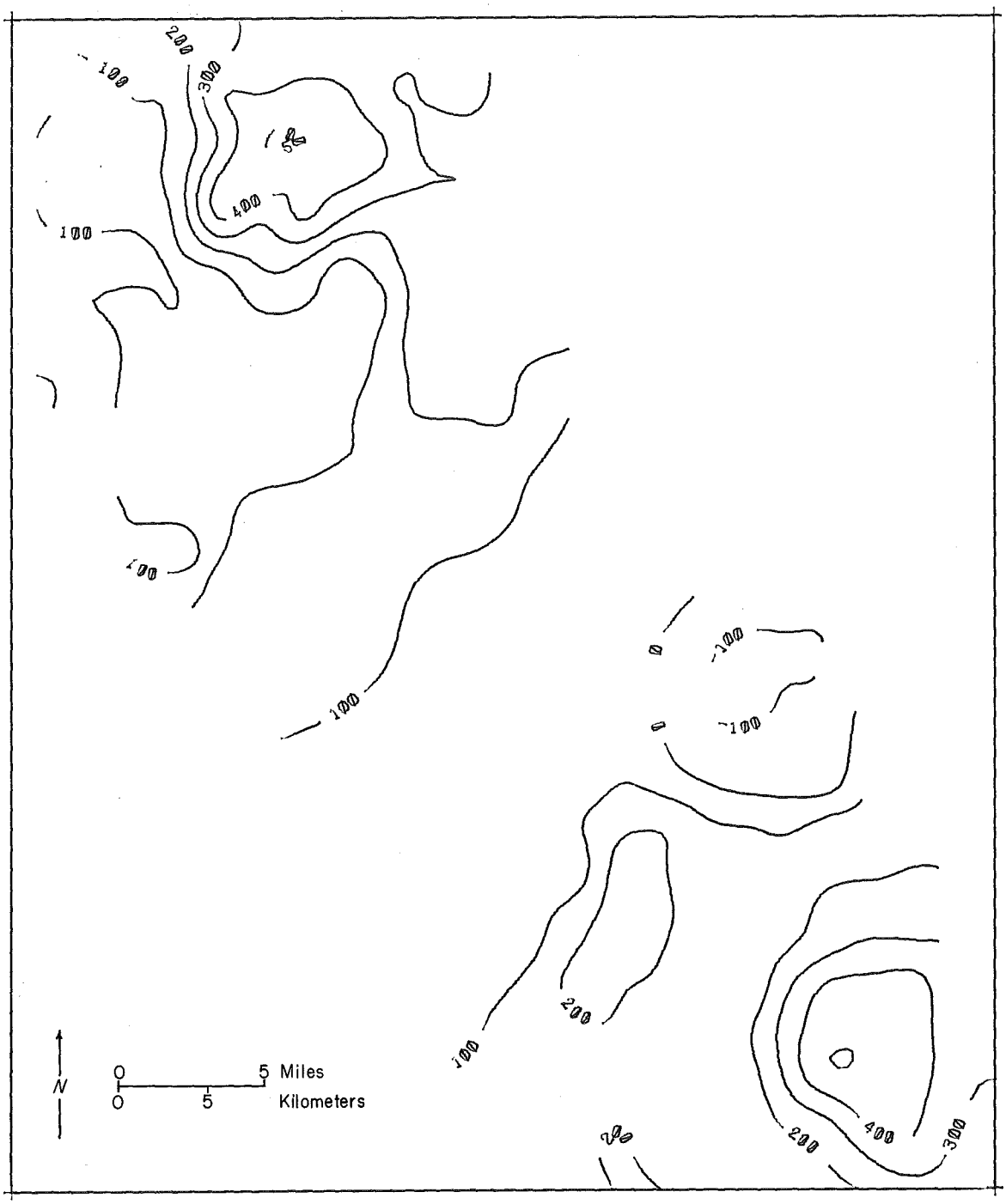

Figure 7. San Pedro: Computer contour map of geothermal gradients; gradients have been calculated in $^{0}C/km$.

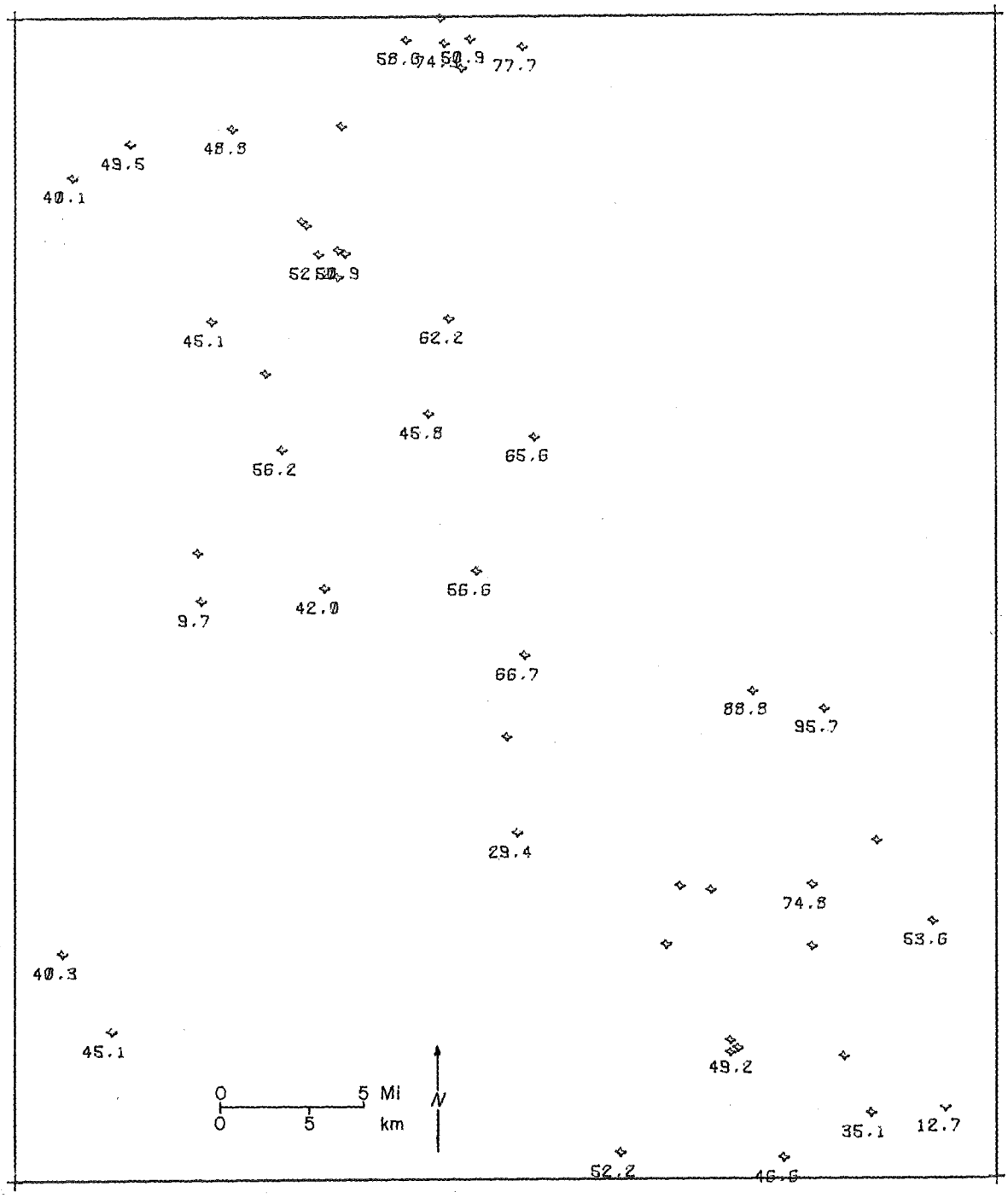

Figure 8. San Pedro: SiO_2 geothermometer temperatures in ^{o}C.

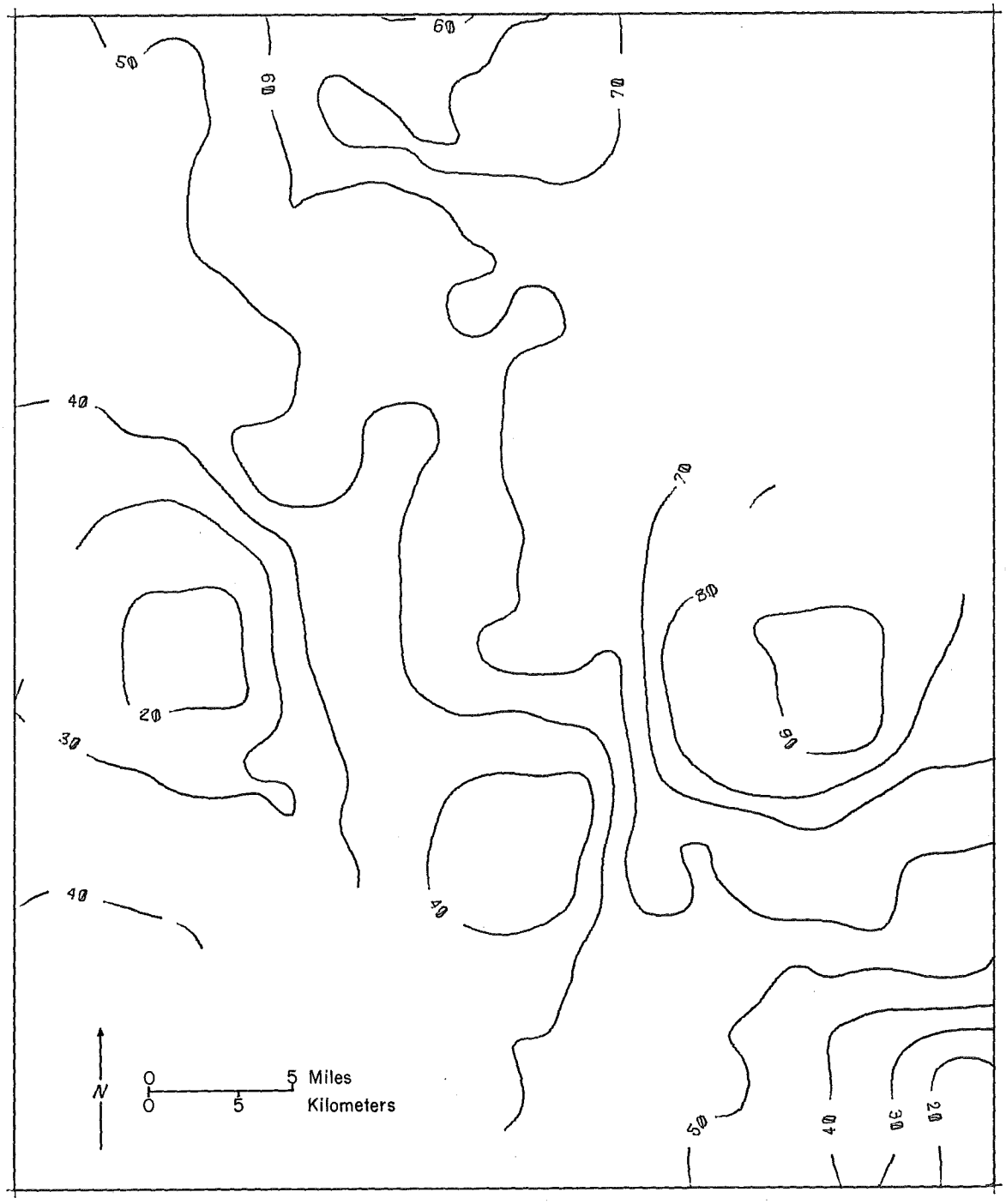

Figure 9. San Pedro: Computer contour map of SiO_2 geothermometer temperatures in ^{o}C.

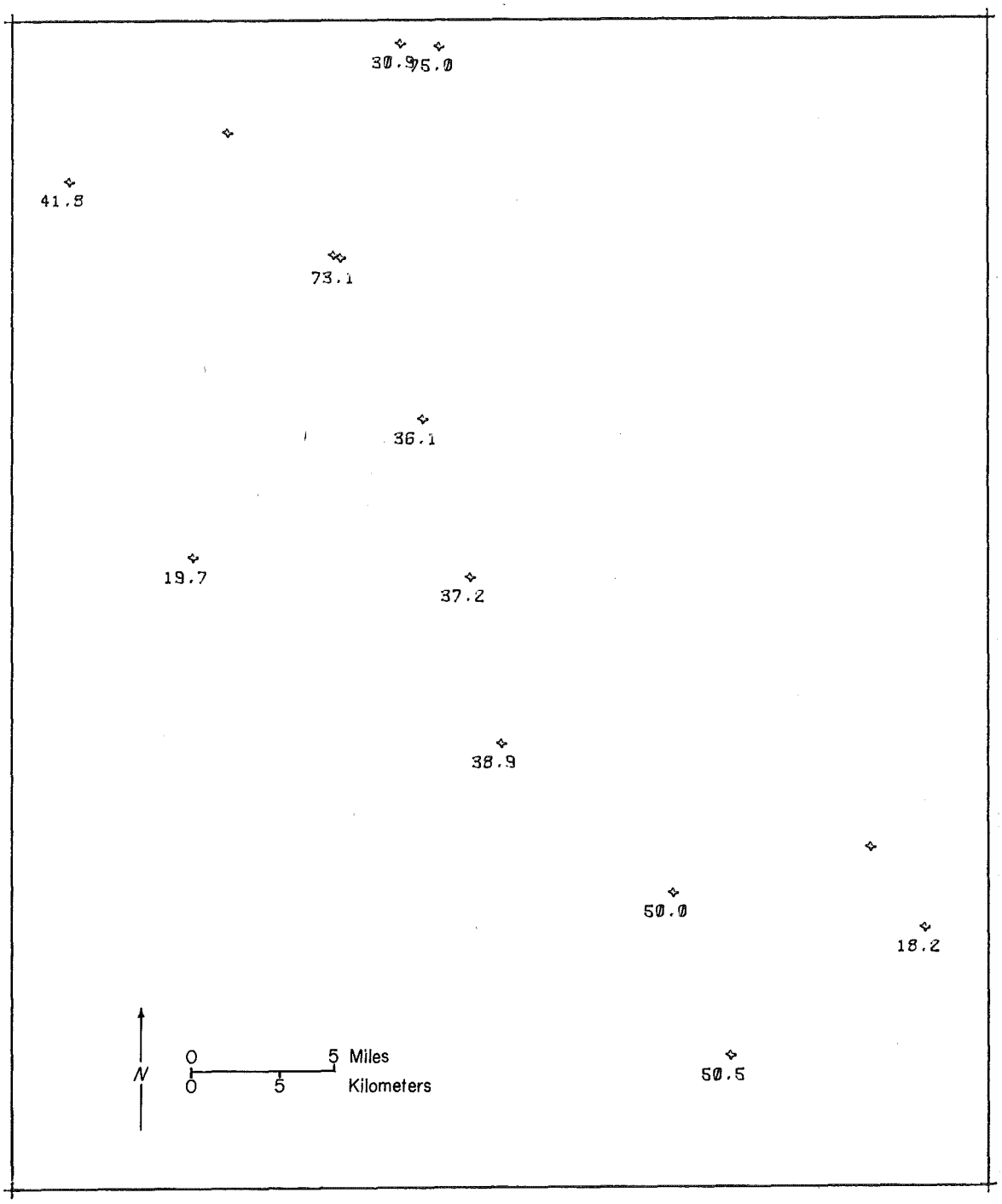

Figure 10. San Pedro: Na-K-Ca geothermometer temperatures in ^{o}C.

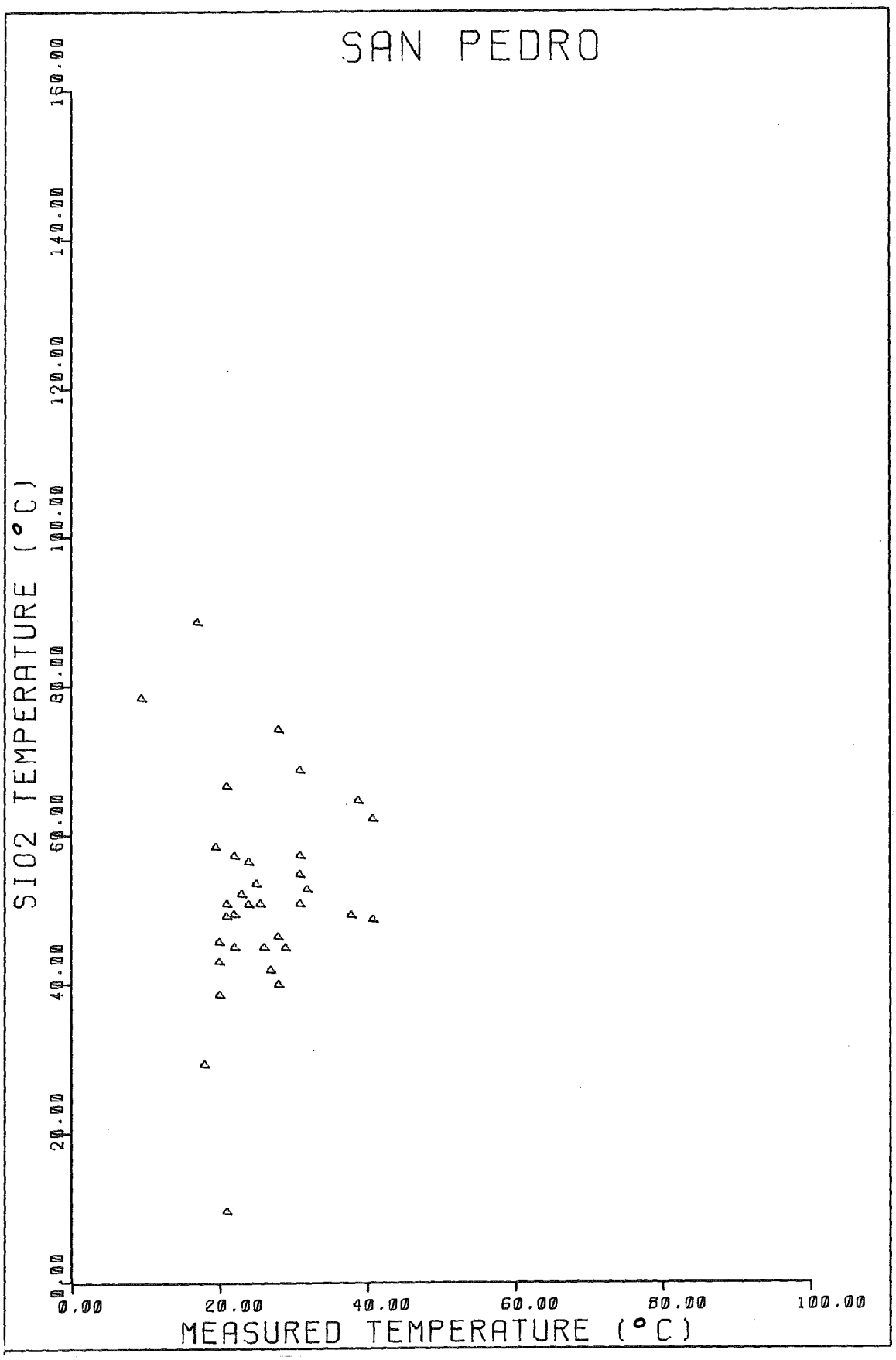

Figure 11. San Pedro: Computer plot of SiO_2 geothermometer versus the measured well discharge temperature.

Table 7
Chemical Analyses, con't.
Hookers Hot Springs

CO_3	HCO_3	Cl	SO_4	SiO_2	F	Li	B	TDS	Geology	Sample #
34	80	9	2	51	1.85	0.14	0.45	180	Volcanoclastic sediment Tertiary age	3W80
42	88	6	3	51	2.61	0.11	0.86	169	Volcanoclastic sediment Tertiary age	4W80
30	78	6	3	54	2.55	0.12	0.35	178	Volcanoclastic sediment Tertiary age	5W80
0	299	12	21	79	2.61	0.22	0.85	428	Volcanoclastic sediment Tertiary age	6W80
40	66	8	1	47	2.15	0.10	0.85	157	Volcanoclastic sediment Tertiary age	7W80
24	76	7	2	47	1.52	0.10	0.50	159	Volcanoclastic sediment Tertiary age	8W80

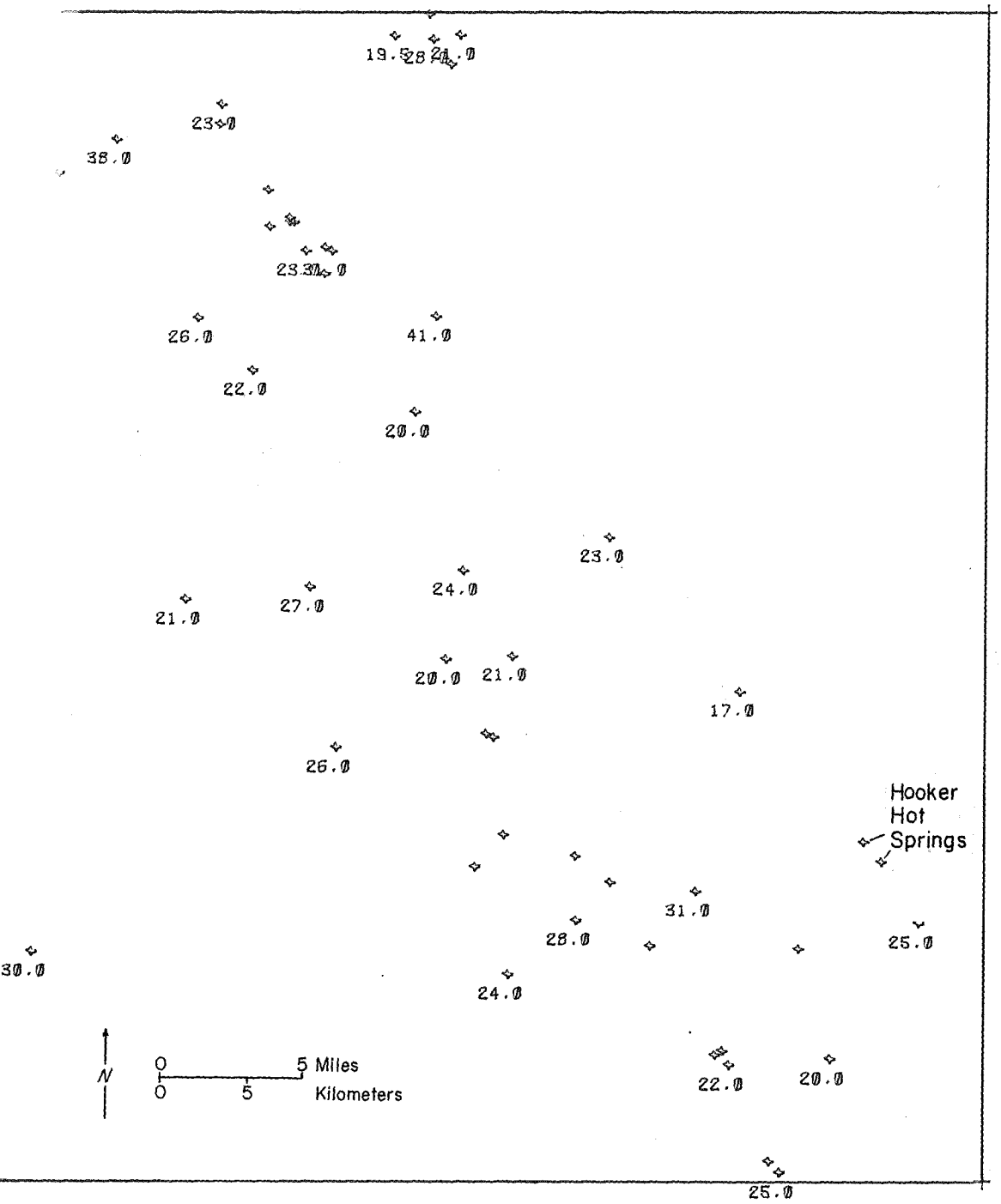

igure 12. San Pedro measured temperatures in ^{o}C.

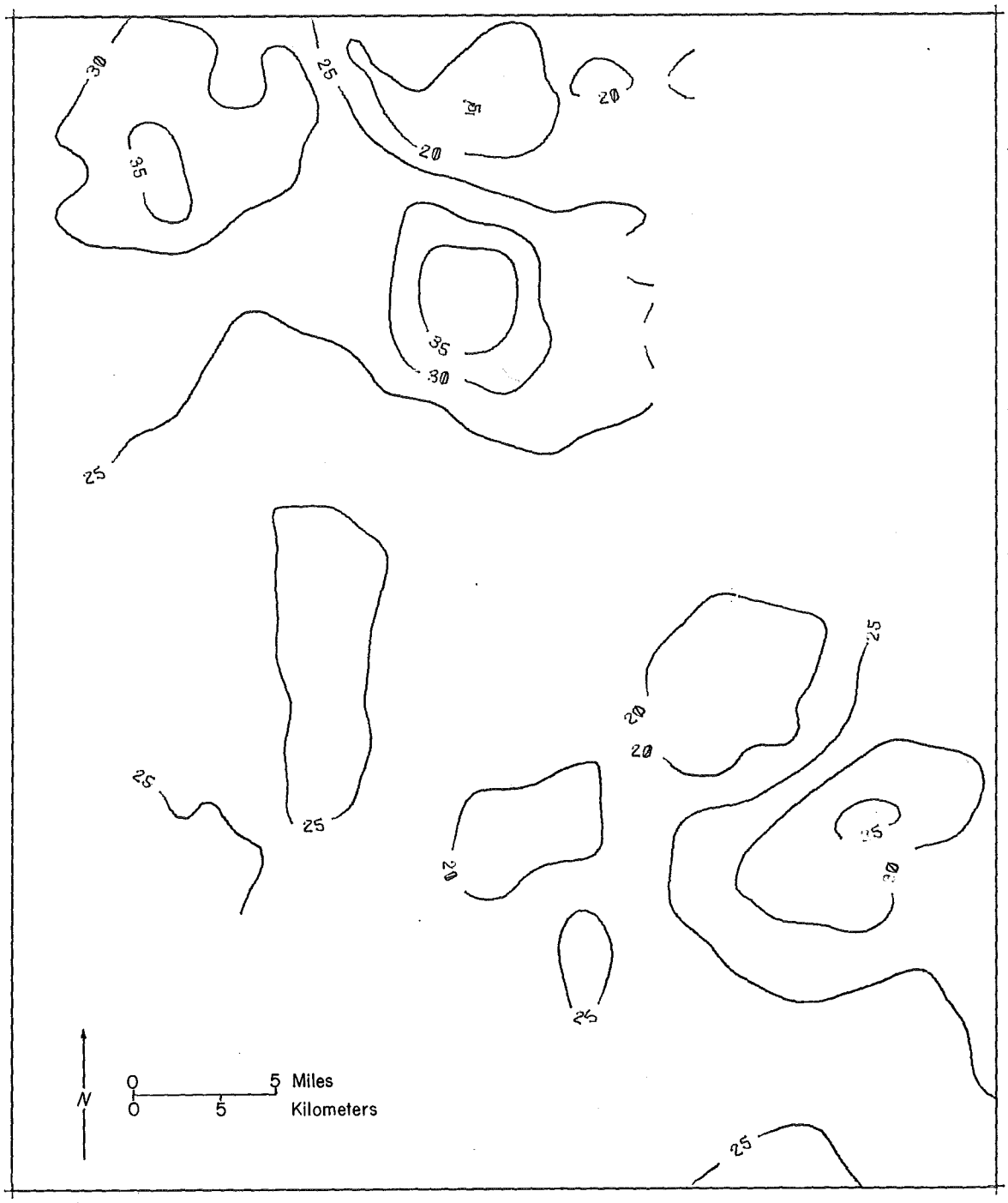

Figure 13. San Pedro: Computer contour map of measured temperatures in ^{o}C.

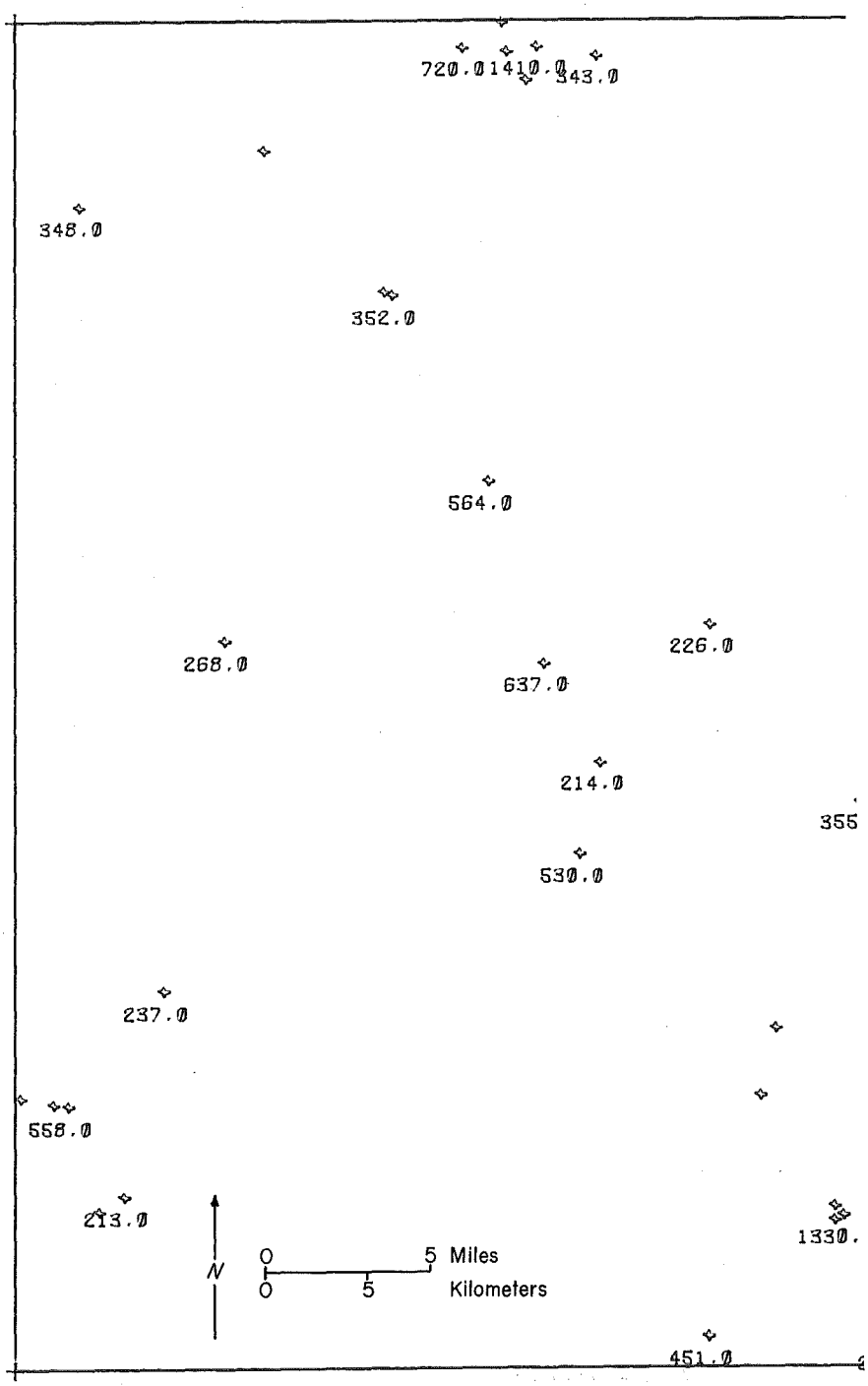

Figure 14. San Pedro: Total dissolved solids (TDS) i
liter (mg/l).

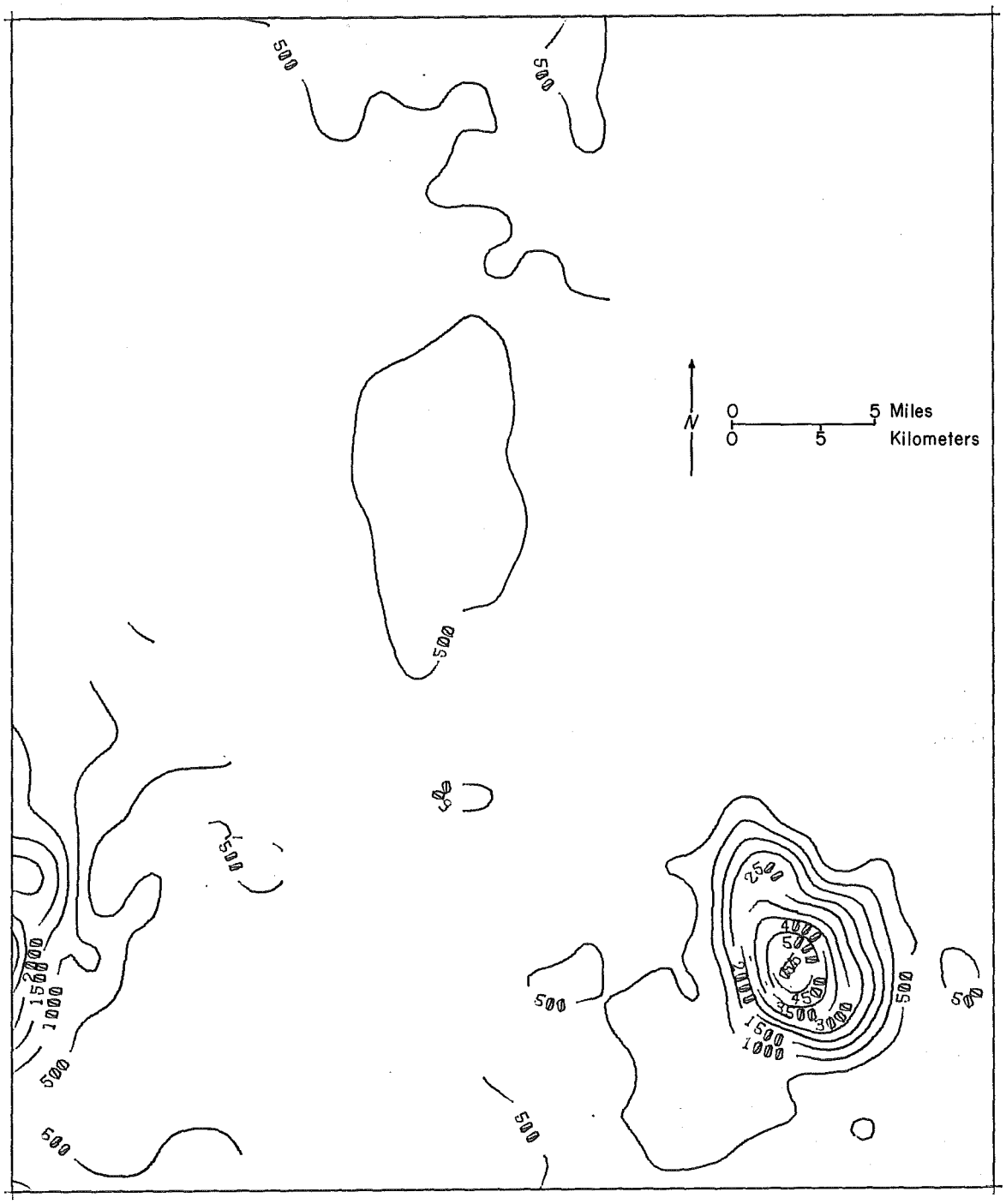

Figure 15. San Pedro: Computer contour map of total dissolved solids (TDS) in milligrams per liter (mg/l).

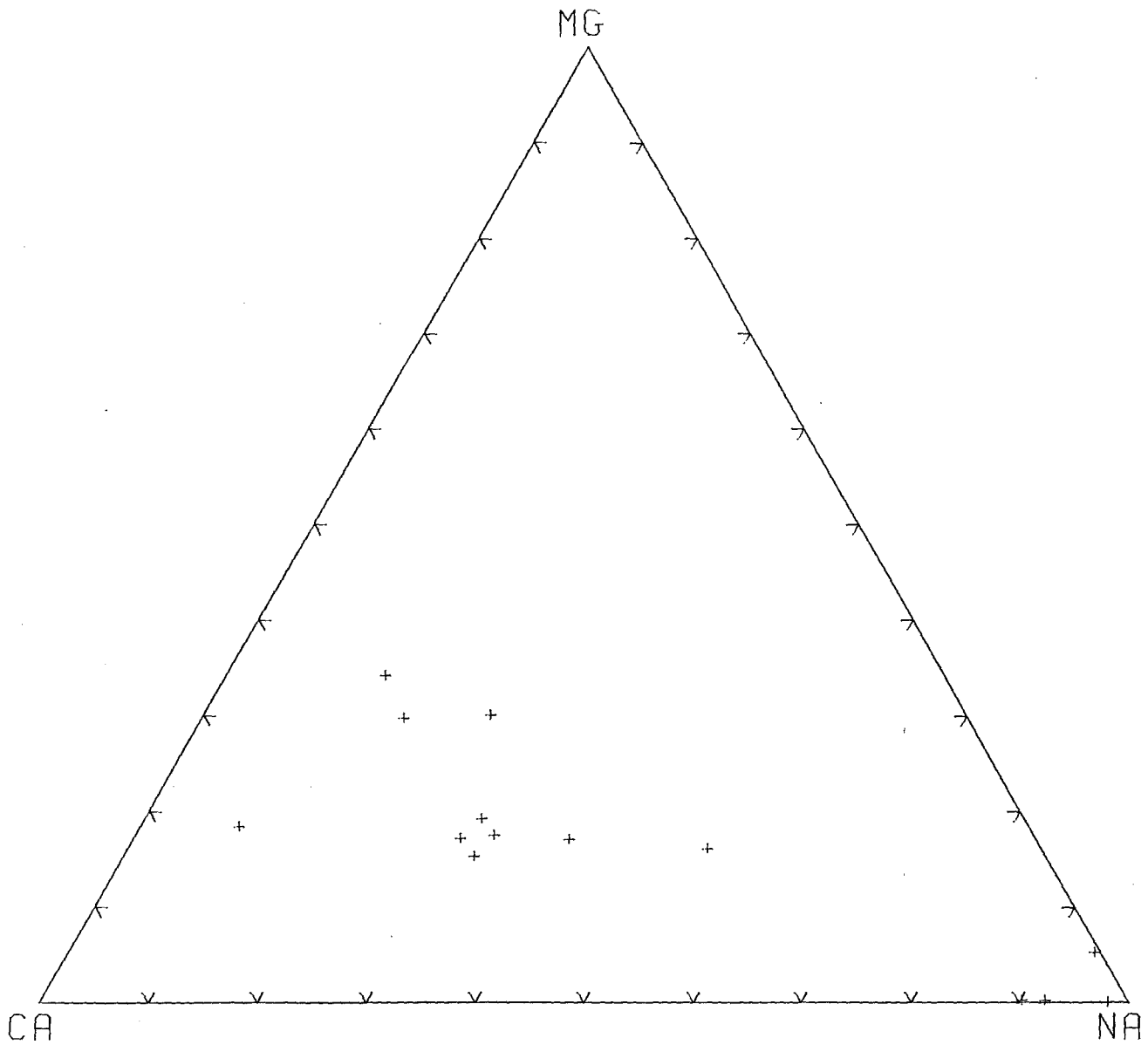

Figure 16. San Pedro triangular diagram of the cations Na-Ca-Mg from available WATSTORE analyses.

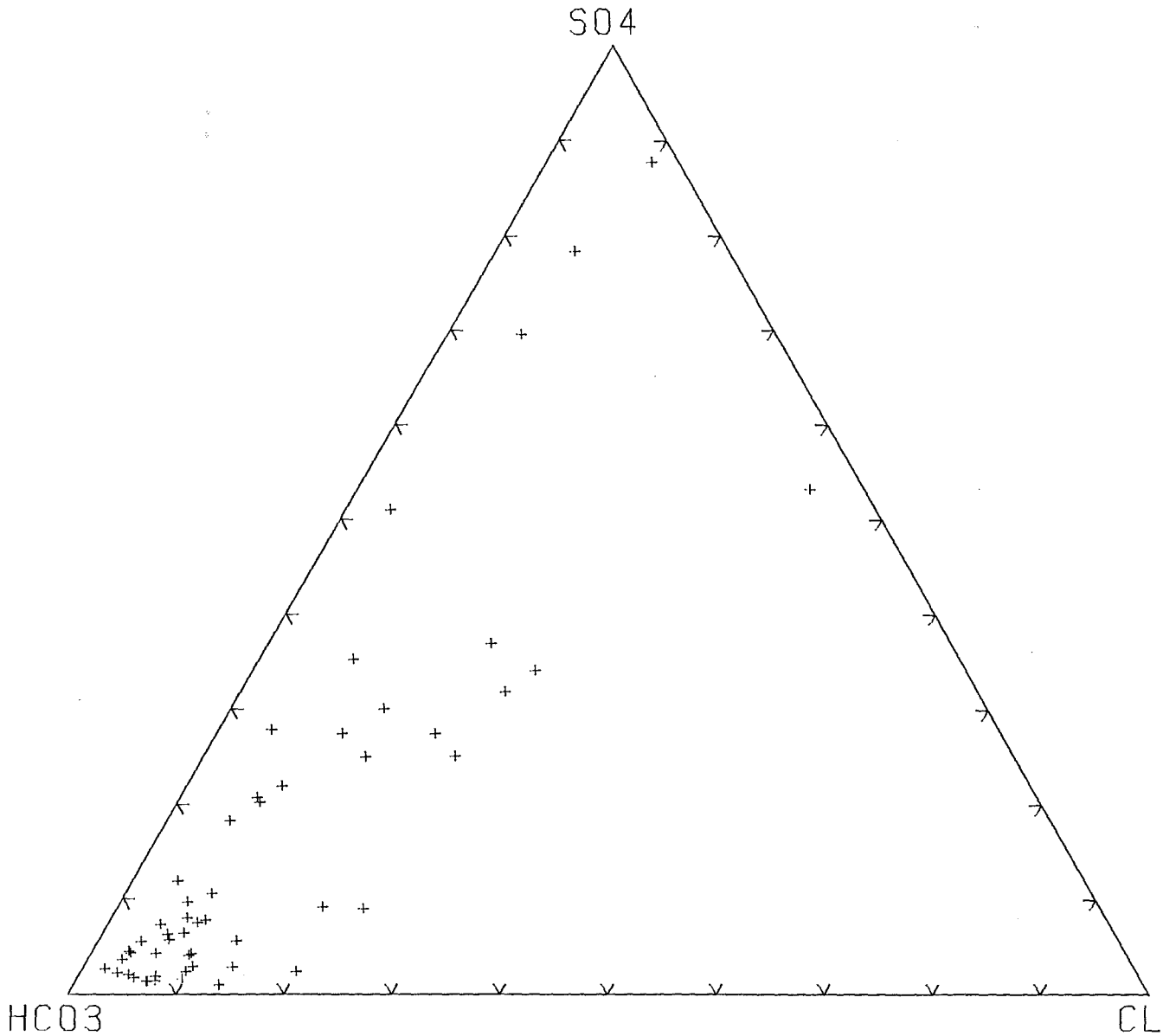

Figure 17. San Pedro triangular diagram of the anions Cl-HCO_3-SO_4 from available WATSTORE analyses.

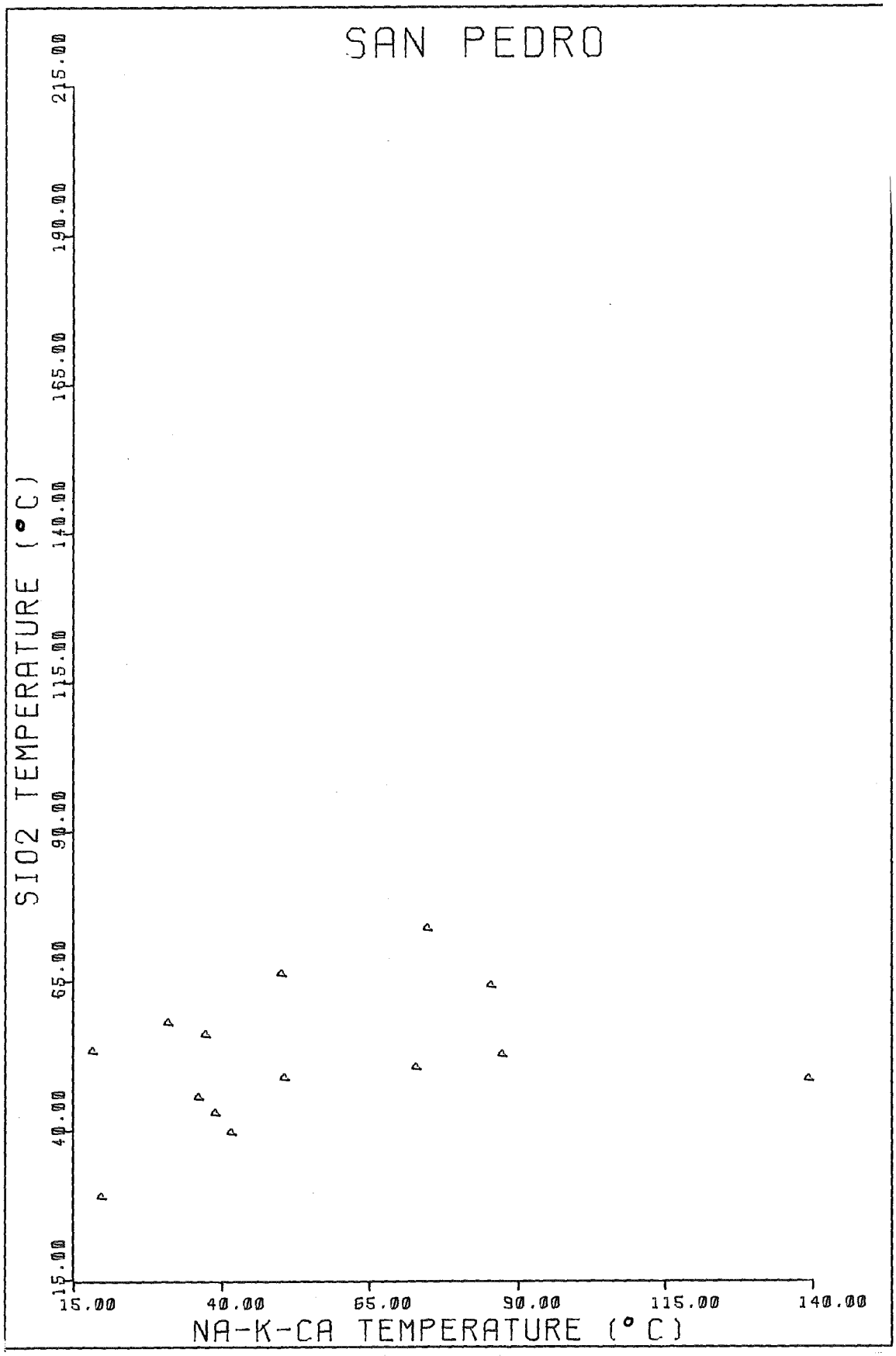

Figure 18. San Pedro: Computer plot of Na-K-Ca geothermometer versus SiO_2 geothermometer.

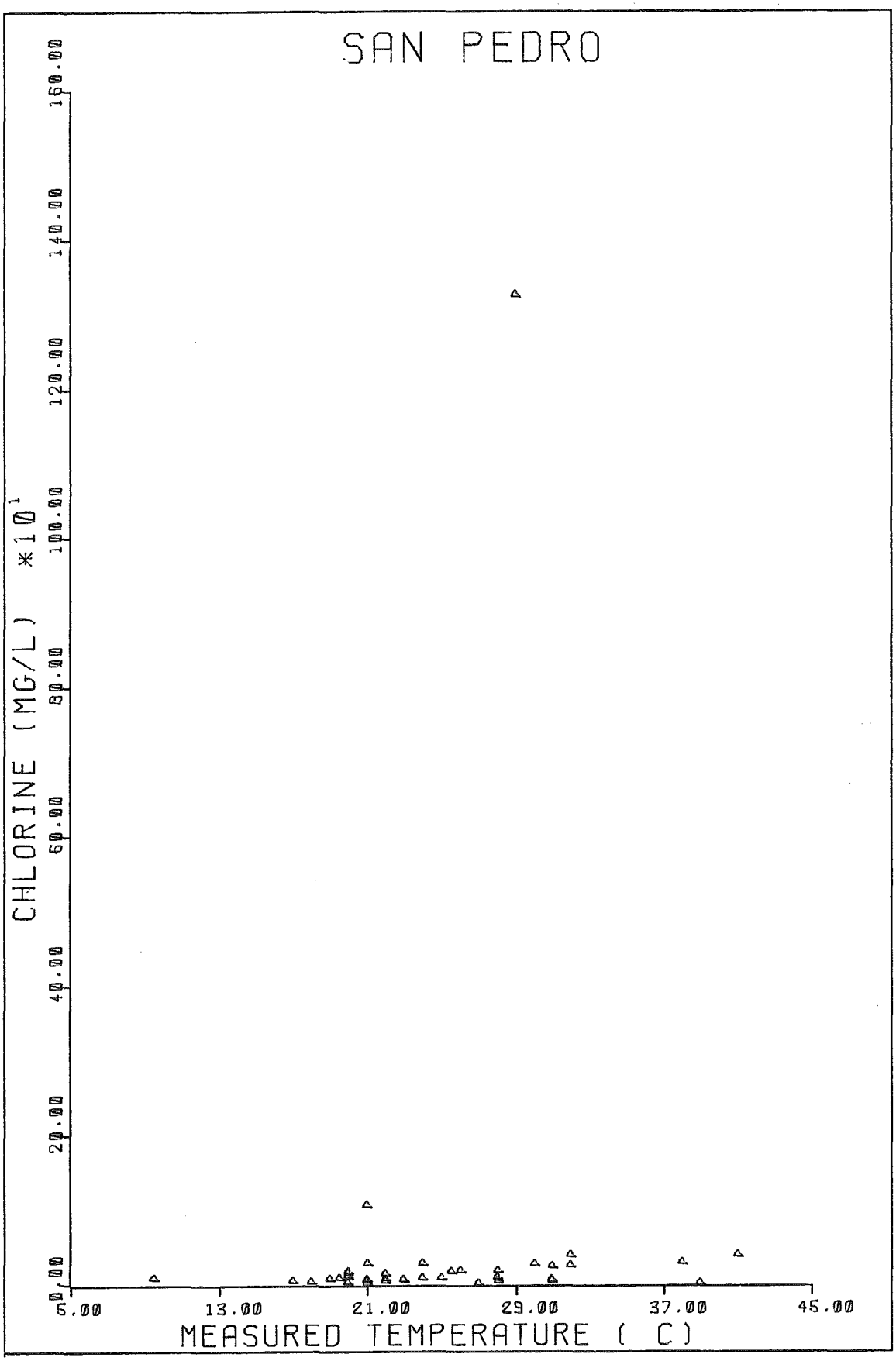

Figure 19. San Pedro: Computer plot of chlorine concentration (mg/l) versus the measured well discharge temperature.

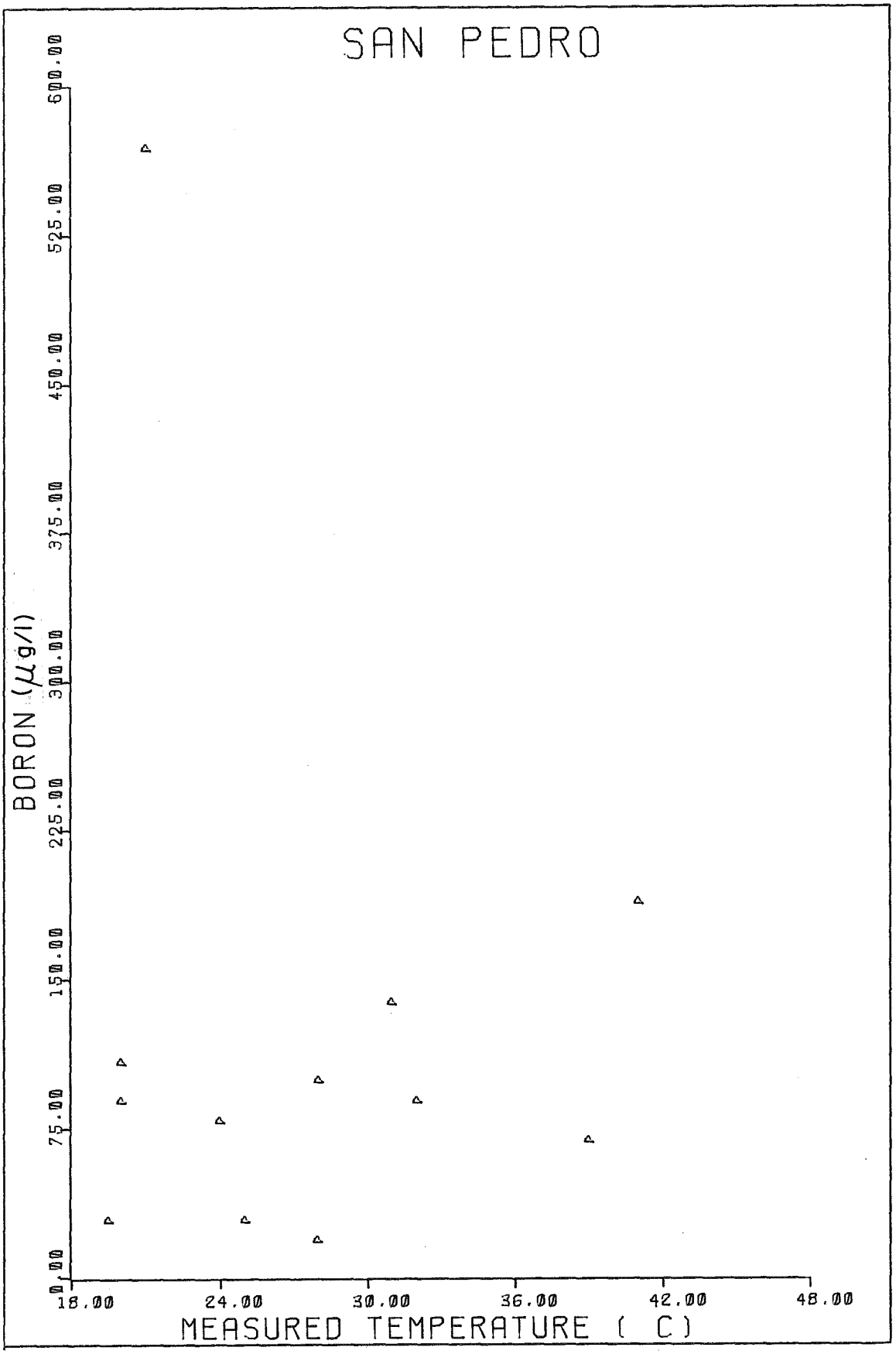

Figure 20. San Pedro: Computer plot of boron concentration (μg/l) versus the measured well discharge temperature.

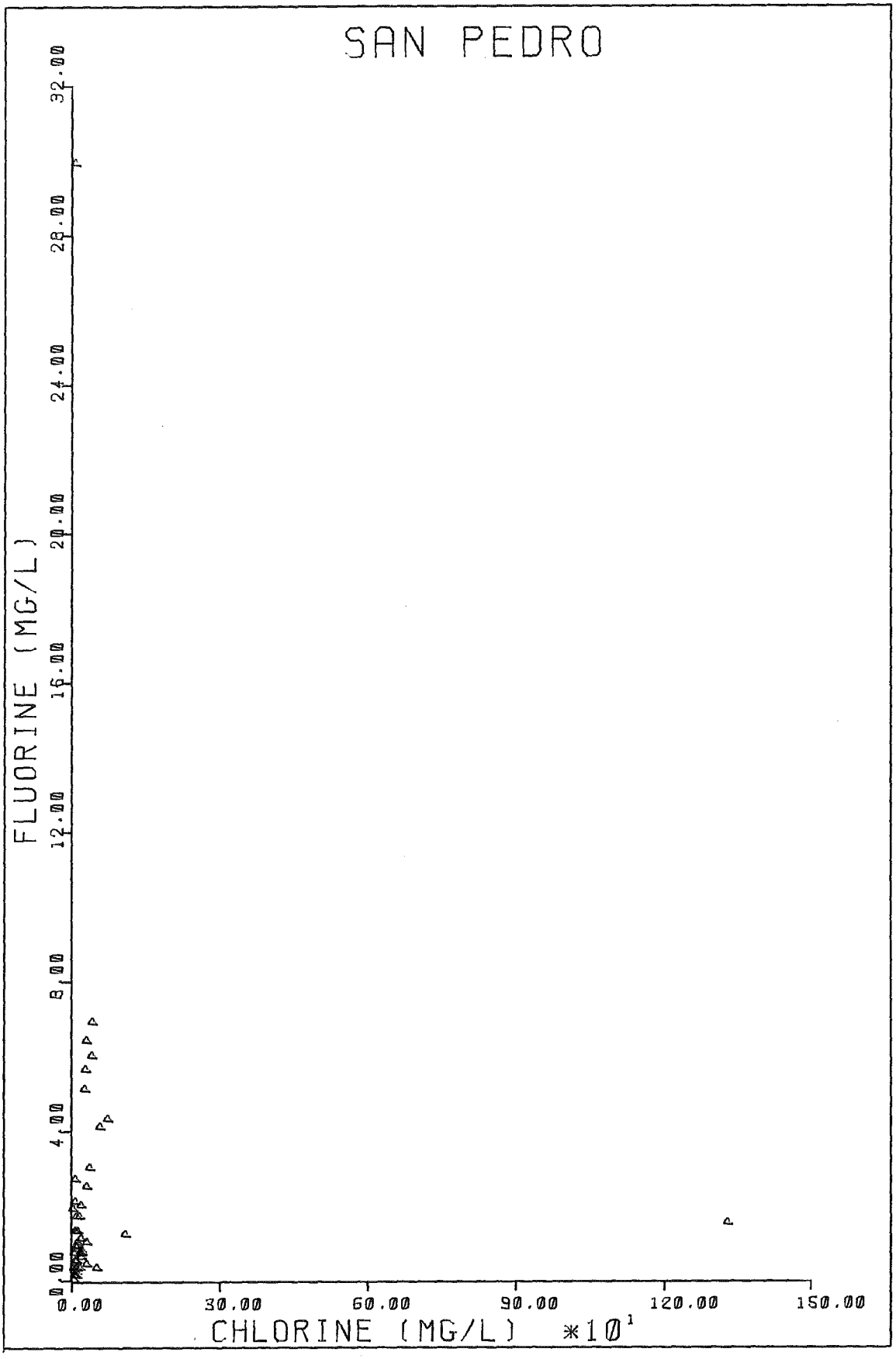

Figure 21. San Pedro: Computer plot of fluorine concentration (mg/l) versus chlorine concentration (mg/l).

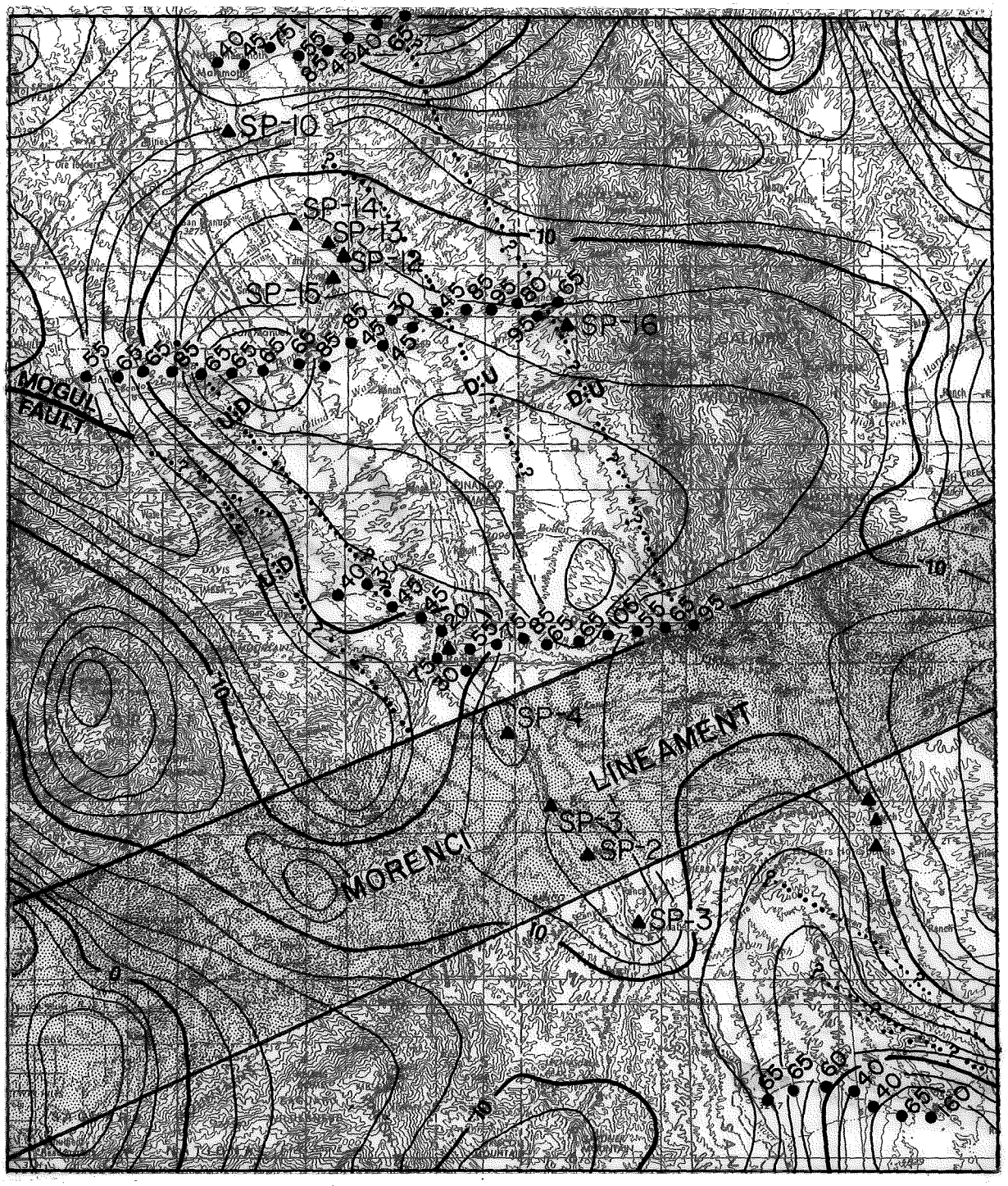

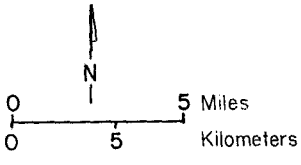

BASE MAP: U.S.G.S. TUCSON, 1:250,000

● MERCURY CONTENT (ppb)

▲ WELL LOCATIONS

?.....? Postulated and inferred faults

Bouguer Gravity

10 mgal contour

2 mgal contour

Figure 22.